



Natural Resources
Canada

Ressources naturelles
Canada

**GEOLOGICAL SURVEY OF CANADA
OPEN FILE 8258**

**Fibre Bragg grating and Brillouin optical time domain
reflectometry monitoring manual
for the Ripley Landslide,
near Ashcroft, British Columbia**

D. Huntley, P. Bobrowsky, Q. Zhang, X. Zhang, and Z. Lv

2017



Canada



GEOLOGICAL SURVEY OF CANADA OPEN FILE 8258

Fibre Bragg grating and Brillouin optical time domain reflectometry monitoring manual for the Ripley Landslide, near Ashcroft, British Columbia

D. Huntley¹, P. Bobrowsky², Q. Zhang³, X. Zhang³, and Z. Lv³

¹ Geological Survey of Canada, 1500-605 Robson Street, Vancouver, British Columbia V6B 5J3

² Geological Survey of Canada, 9860 West Saanich Road, Sidney, British Columbia V8L 5T5

³ Centre for Hydrology and Environmental Geology, China Geological Survey, Baoding, Hubei, China

2017

© Her Majesty the Queen in Right of Canada, as represented by the Minister of Natural Resources, 2017

Information contained in this publication or product may be reproduced, in part or in whole, and by any means, for personal or public non-commercial purposes, without charge or further permission, unless otherwise specified.

You are asked to:

- exercise due diligence in ensuring the accuracy of the materials reproduced;
- indicate the complete title of the materials reproduced, and the name of the author organization;
- indicate that the reproduction is a copy of an official work that is published by Natural Resources Canada (NRCan) and the Geological Survey of Canada (GSC); and
- indicate that the reproduction has not been produced in affiliation with, or with the endorsement of NRCan.

Commercial reproduction and distribution is prohibited except with written permission from NRCan. For more information, contact NRCan at nrcan.copyrightdroitdauteur.nrcan@canada.ca

Permanent link: <https://doi.org/10.4095/304235>

Recommended citation

Huntley, D., Bobrowsky, P., Zhang, Q., Zhang X. and Lv, Z. 2017. Fibre Bragg grating and Brillouin optical time domain reflectometry monitoring manual for the Ripley Landslide, near Ashcroft, British Columbia; Geological Survey of Canada, Open File 8258, 66 p. <https://doi.org/10.4095/304235>

Publications in this series are critically reviewed by scientific peers and released as submitted by the authors. This Open File has not been edited.

Table of Contents

Abstract	5
Preface	6
<i>Keywords</i>	6
1. Introduction	7
1.1 <i>Aim of publication</i>	8
2. Conventional Monitoring Instrumentation at the Ripley Test Site	9
2.1 <i>Limitations to Vibrating-Wire Instrumentation and Advantages of Fibre Optic Technologies</i>	9
3. Fibre Optic Monitoring Technologies tested at the Ripley Landslide	9
3.1 <i>Background on Fibre Optic Technologies</i>	9
3.2 <i>Fibre Optic Monitoring Design</i>	10
3.3 <i>Installation of the BOTDR and FBG Sensor Layouts</i>	10
3.4 <i>Initial Operational Procedures for FBG and BODTR systems</i>	13
4. Optical Fibre Grating Monitoring Demodulation (FBG) Device	15
4.1 <i>Technical specifications</i>	15
4.2 <i>Operating FBG Modulation Software</i>	16
4.3 <i>Manual Measurement Mode</i>	17
4.4 <i>Dynamic Interface</i>	19
4.5 <i>Set Parameters Interface</i>	20
4.6 <i>Test Results Interface</i>	24
4.7 <i>Acquisition Time Setting Interface</i>	25
4.8 <i>Exit View</i>	26
4.9 <i>Automatic Measurement Mode</i>	26
5. Distributed Fibre Optic Strain (BOTDR) Monitoring System	28
5.1 <i>Acquisition software interface and acquisition process</i>	29
5.2 <i>System data receiving software</i>	31
6. Data Monitoring Platform	32
6.1 <i>Logging into the monitoring platform</i>	32
6.2 <i>FBG data monitoring</i>	34
6.3 <i>BOTDR data monitoring</i>	37
6.4 <i>Data management</i>	41
6.5 <i>Document scanning and system management</i>	43
6.6 <i>FBG monitoring time maintenance module</i>	43
6.7 <i>BOTDR monitoring time maintenance</i>	45
6.8 <i>Trouble-shooting FBG and BOTDR instruments at the Ripley Landslide test site</i>	46
7. Optical Fibre Sensing Real-Time Monitoring Results and Interpretations	48
7.1 <i>FBG and BODTR results</i>	48
7.2 <i>Interpretation of FBG and BODTR data</i>	49

8. Concluding Remarks	51
<i>8.1 Summary evaluation of fibre-optic cable technologies</i>	
<i>8.2 Limitations</i>	51
<i>8.3 Applications</i>	51
9. Acknowledgements	52
10. References	52
APPENDIX 1	
Detailed list of items for the China-Canada optical fibre real-time monitoring project	55
APPENDIX 2	
Fibre Bragg Grating Installation and Operation: Quick View	56
APPENDIX 3	
Brillouin Optical Time Domain Reflectometry Installation and Operation: Quick View ..	58
APPENDIX 4	
Optical Time Domain Reflectometry Repair Operation: Quick View	59
APPENDIX 5	
Welding Fibre Optic Cable Operation: Quick View	60

Fibre Bragg grating and Brillouin optical time domain reflectometry monitoring manual for the Ripley Landslide, near Ashcroft, British Columbia

D. Huntley¹, P. Bobrowsky², Q. Zhang³, X. Zhang³, and Z. Lv³

1. Geological Survey of Canada, 1500-605 Robson Street, Vancouver, British Columbia V6B 5J3
2. Geological Survey of Canada, 9860 West Saanich Road, Sidney, British Columbia V8L 5T5
3. Centre for Hydrology and Environmental Geology, China Geological Survey, Baoding, Hubei, China

Abstract

An international multi-year project is investigating and monitoring the Ripley Landslide, 7 km south of Ashcroft, British Columbia. The aim of this collaborative work is to better understand and manage landslides along Canada's western railway corridor. From 2013 to 2016, the China Geological Survey (CGS) and Geological Survey of Canada (GSC) collaborated to test and evaluate experimental fibre Bragg grating (FBG) and Brillouin optical time domain reflectometry (BOTDR) technologies on an active landslide for the first time in Canada. Open File 8258 describes the operational procedures for these monitoring systems. FBG and BOTDR monitoring systems were installed on a lock-block retaining wall that separates the Canadian National (CN) and Canadian Pacific Railway (CP) tracks. This vital component of railway infrastructure crosses the southern extent of the main slide body; and was monitored with the aims of better understanding the deformation mechanisms and potential triggers for sudden movement; and managing the risks associated with railway operations. Monitoring data was processed on site then accessed by wireless transmitter from remote terminals at the CGS and GSC offices. Results, discussed in the context of interpretations from other physical surveys of the landslide, provide new insight into the nature and distribution of surficial earth materials, their stratigraphic relationships, internal structure of the landslide, and structural integrity of critical railway infrastructure. This study demonstrates that optical fibre sensing real-time techniques are viable, cost effective monitoring methods that can ensure the safety and security of the railways, thereby reducing risks to national public safety, the environment, natural resources and international economies.

Preface

A four-year cooperative project from 2013 to 2016 was undertaken at the Ripley Landslide near Ashcroft, British Columbia as part of a Memorandum of Understanding and Project ANNEX between the Government of Canada, through the Geological Survey of Canada (GSC) and the Government of China, through the China Geological Survey (CGS). The Ripley Landslide Project is an International Activity under NRCAN's Public Safety and Geoscience Program. This project aims to gain a better understanding of the landslides in the Thompson River valley and to help reduce the risks they pose to the railways operating in this critical section of Canada's transportation corridor through the western Cordillera.

Key activity partners include Transport Canada, the Department of Civil Engineering at University of Alberta (UA), Canadian National (CN) and Canadian Pacific (CP) railways, collectively grouped in the Railway Ground Hazard Research Program (RGHRP). An element of collaborative research and development for the Ripley Landslide Project involved the adaption of state-of-the-art landslide fibre optic monitoring technologies now widely used in China and testing their application in Canada. In April-May 2013, the GSC hosted a 10-day field program near Ashcroft, Canada with colleagues from the CGS to install innovative remote monitoring systems on an active landslide that poses a significant risk to the national railway transportation corridor in south-central British Columbia. A follow-up workshop at CHEGS in Baoding, PRC in March 2014 focused on field technical exchange and training to repair and use the fibre optic equipment donated by the CGS for the duration of the project.

These training workshops will help to further the partnership and understanding of the capabilities in the two organizations. Direct interchange through fieldwork, conference presentations and laboratory training exercises were fundamental to the project and for ensuring effective long-term collaboration. Scientists from Canada and China greatly benefitted from this technical exchange and this collaboration was an unprecedented opportunity to learn and improve upon the experience of others. Through their combined efforts, the GSC, CGS and RGHRP are improving the safety of operation, reducing the potential for national railway service interruptions and loss of other critical infrastructure: all closely linked with the performance of the global economy and public safety.

Keywords

Ripley Landslide, British Columbia, Fibre Bragg Grating, Brillouin Optical Time Domain Reflectometry, Real-Time Monitoring, Geological Survey of Canada, China Geological Survey

1. Introduction

Landslides in the mountain valleys of western Canada have challenged the development and operation of railways since the late 19th Century. At present, pronounced economic and environmental repercussions can occur when rail service is disrupted by landslide activity. A vital section of the national railway transportation corridor runs through the Thompson River valley in southern British Columbia. This is a unique area where complex glacial geology, active geomorphic processes and rail infrastructure intersect and are affected by slope instability for many decades (**Figure 1a**). There are three possible strategies to reduce the risks associated with landslides in this corridor. Avoiding landslide-prone terrain is not possible for CN and CP tracks in the valley. Stabilizing landslides is prohibitively costly, and geotechnical problems preclude this option. Identifying landslide-prone terrain and monitoring for unsafe ground movement is the most cost-effective risk management approach for railway companies and government agencies in the valley (Bunce and Chadwick 2012). Adopting this third strategy, an international consortium of research partners has embarked upon a detailed multi-year study to investigate and monitor the active Ripley Landslide, 7 km south of Ashcroft, British Columbia in a collective effort to better understand and manage this, and by extension, other landslide hazards in Canada and elsewhere (Bobrowsky et al. 2014; **Figure 1a, b**).

A shift from geohazard monitoring using vibrating wire sensors to the widespread application of fibre optic technologies has taken place over the last 20 years. Theoretical and experimental fibre optic sensing technologies have been developed at various institutions and universities in China for monitoring critical transportation and energy infrastructure (e.g., measuring the structural integrity of bridges and dams) since the 1990's. In this century, fibre optic sensing technology has been applied to the dynamic monitoring of landslides in China, India, Europe, South America and United States (e.g., Huang et al. 2002; Yoshida et al. 2002; Yong et al. 2005; Laudati et al. 2007; Hoepfner et al. 2008; Wang et al. 2008; Huaifu et al. 2011; Huang et al. 2012). Most recently, the China Geological Survey (CGS) has developed and field-tested an array of fibre optic sensing technologies developed for extreme environments, for example the Three Gorges Reservoir area (Xu et al. 2007; Wang et al. 2009).

From 2013 to 2016, the China Geological Survey (CGS) and Geological Survey of Canada (GSC) collaborated to test and evaluate experimental fibre Bragg grating (FBG) and Brillouin optical time domain reflectometry (BOTDR) technologies on an active landslide for the first time in Canada (Zhang et al. 2014; Huntley et al. 2016). Innovative real-time fibre optic monitoring systems were installed on a lock-block retaining wall that separates the Canadian National (CN) and Canadian Pacific Railway (CPR) tracks. This vital component of railway infrastructure crosses the southern extent of the main slide body; and was monitored with the aims of better understanding the deformation mechanisms and potential triggers for sudden movement; and managing the risks associated with railway operations.

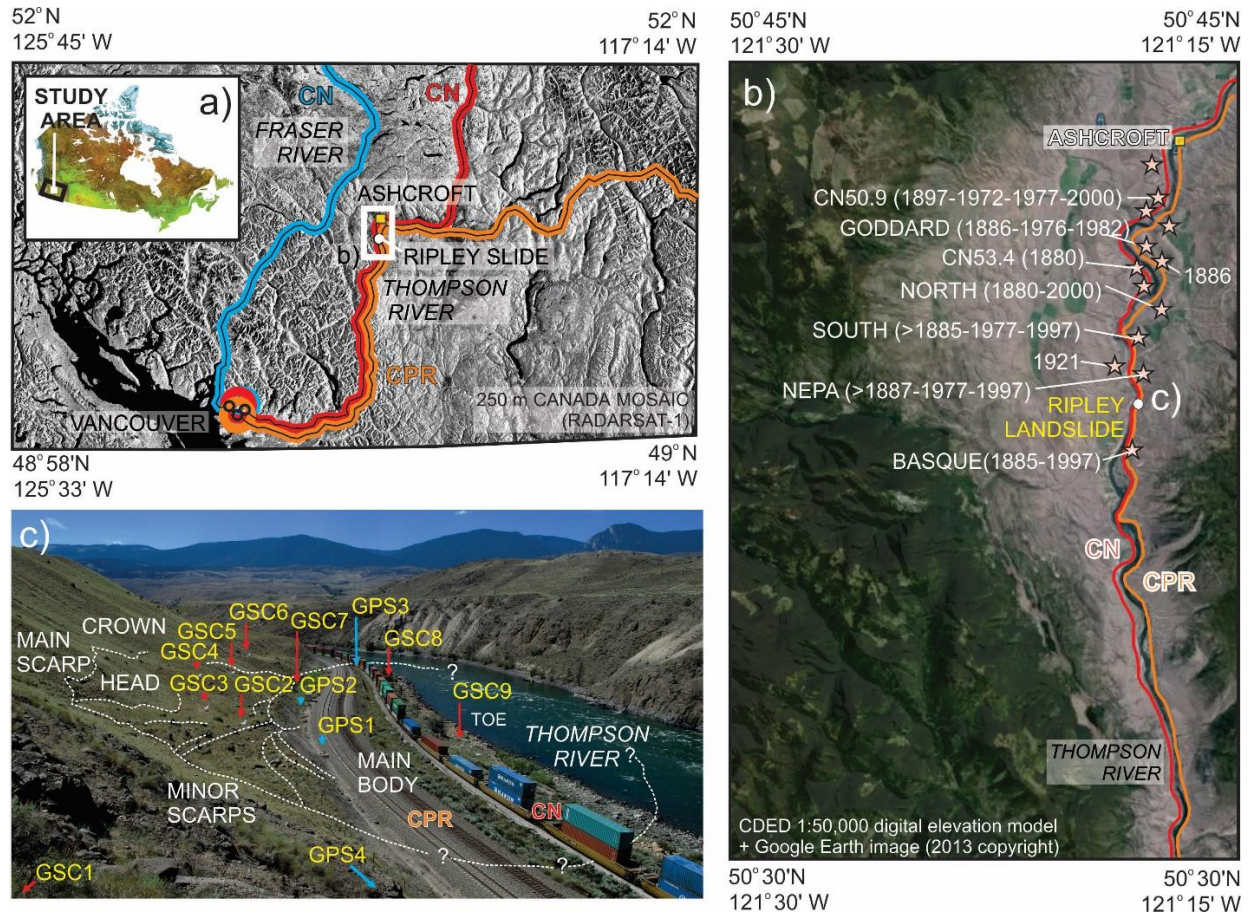


Figure 1 Location of the Ripley Landslide, also showing: a) Rail transportation corridors in southwestern British Columbia with location of Ripley Landslide test site; b) Landslides of the Thompson River valley rail transportation corridor with location of Ashcroft and the Ripley Landslide test site; c) Overview of the Ripley Landslide test site highlighting the location of GPS monitoring stations (GPS1-4), InSAR corner reflectors (GSC1-9), and the monitored retaining wall dividing the CN and CPR tracks - view to south.

1.1 Aim of publication

This Open File manual is a user's guide to the installation and operation of the FBG and BODTR systems installed at the Ripley Landslide test site (**Figure 1c**) from March 2013 to November 2015. Monitoring data were processed on site then accessed by wireless transmitter from remote terminals at the CGS and GSC offices. Results, discussed in the context of interpretations from other physical surveys of the landslide, provide new insight into the nature and distribution of surficial earth materials, their stratigraphic relationships, internal structure of the landslide, and structural integrity of critical railway infrastructure (e.g., Huntley et al. 2014a; Huntley et al. 2014a; Huntley et al. 2016). This study demonstrates that despite installation setbacks and extreme environmental conditions, optical fibre sensing real-time techniques are viable monitoring methods that can help ensure the safety and security of the railways, thereby reducing risks to public safety, the environment, natural resources and the economy.

2. Conventional Monitoring Instrumentation at the Ripley Test Site

Surficial geology mapping and borehole logging, combined with waterborne and terrestrial electrical resistivity tomography, electromagnetic conductivity, seismic refraction, shear wave, natural gamma radiation, induction conductivity and magnetic susceptibility surveys provide insight into the composition and structure of the landslide (Huntley and Bobrowsky 2014; Huntley et al. 2017a; 2017b). Additionally, a number of conventional and experimental continuous monitoring technologies have been installed on site. Subsurface monitoring of boreholes drilled in 2013 and 2015 include ShapeAccelArray inclinometry and piezometer head levels (Schafer et al. 2015). River elevations are calibrated with flow rates from a nearby monitoring station (Hendry et al. 2015). Ground displacement is monitored at four permanent global positioning system (GPS) stations installed across the main body of the landslide and adjacent stable bedrock (Bunce and Chadwick 2012); and with passive interferometric synthetic aperture radar (InSAR) reflectors installed for satellite-based (RADARSAT-2) interferometry (Bobrowsky et al. 2014; Macciotta et al. 2014; Huntley et al. 2017c).

2.1 Limitations to Vibrating-Wire Instrumentation and Advantages of Fibre Optic Technologies

For the Ripley Landslide test site, borehole and GPS installations use conventional vibrating wire piezometers, inclinometers, strain gauges, accelerometers and geophones that require a large number of cables per installation; experience electromagnetic interference and signal degradation with long distance transmission; and generally have poor long-term reliability (e.g., Bunce and Chadwick 2012; Hendry et al. 2015; Schafer et al 2015). In contrast, sensor systems using optical glass fibre cable do not have these limitations, making them reliable for monitoring strain and pore water pressure in landslides. In addition to being more cost effective, fibre optic systems also have performance advantages including higher data resolution and faster sampling rates (e.g., Huang et al. 2002; Yoshida et al. 2002; Yong et al. 2005; Laudati et al. 2007; Wang et al., 2008; Wang et al. 2009, Huaifu et al. 2011).

3. Fibre Optic Monitoring Technologies tested at the Ripley Landslide

Between 2013 and 2016, the CGS and Geological Survey of Canada (GSC) collaborated to install, test and evaluate experimental fibre Bragg grating (FBG) and Brillouin optical time domain reflectometry (BOTDR) technologies for the first time on an active landslide in Canada (**Figure 1a**). For this study, strain and temperature was monitored in the deforming lock-block retaining wall separating the CN and CP tracks (**Figure 2c**) using a combination of FBG and BOTDR technologies (Bobrowsky et al. 2014; Huntley et al. 2014b; Zhang et al. 2014; Huntley et al. 2016).

3.1 Background on Fibre Optic Technologies

Optical time domain reflectometry measures the time intervals between emission and reception of monochromatic laser light pulses with a known propagation velocity emitted to determine

distance to deformed portions of optical fibre cable. Amplitude, width and form of the transmitted, received and reflected signals reveal information about the type and amount of deformation. Distributed strain and temperature can be determined along an optical fibre by measuring the power and frequency shift of Brillouin peaks in the back-scattered frequency spectrum. BOTDR measurements are single-ended so that local strain in the fibre can be evaluated even if the cable is ruptured. However, physical restrictions limit the spatial resolution to 1 m (Hoepfner et al. 2008; Zhang et al. 2014)

FBGs are short segments (<20 mm) of optical cable containing variations in the refractive index of the core glass fibre that when illuminated by a waveband light source (e.g., from a monochromatic laser), results in a fraction of the transmitted light reflected backward to create an interference pattern. The wavelength of the reflected light is linearly related to the longitudinal strain in the FBG optic fibre cable (Huang et al. 2012). A separate FBG monitored temperature variations for calibration and corrections (Zhang et al. 2014).

3.2 Fibre Optic Monitoring Design

The design of the optical fibre real-time landslide monitoring system combined BOTDR, FBG, database management and web server technologies (Bobrowsky et al. 2014; Zhang et al. 2014; Huntley et al. 2014b; Huntley et al. 2016; **Figure 2a; Table 1; Appendix 1**). Installation was undertaken from late April to early May 2013 and overseen by the CGS, GSC, CN and CP. A combination of household epoxy resins, caulking products, foam fillers and rock bolts were used to attach fibre-optic cables and sensors to the concrete blocks (**Figure 2b, c**). The BOTDR monitoring instrument and FBG demodulation device were connected to a central computer through RS232 cables in the CP bungalow (**Figure 2a, d**). The computer was configured with a static IP and internet connectivity. The system computer ran continuously, while BOTDR and FBG monitors acquired data on start-up every few hours before automatically powering down. The computer operated data acquisition software, database storage and the web server program (**Figure 2a; Table 1**). BOTDR and FBG data could be queried and plotted with modem connection to the internet.

3.3 Installation of the BOTDR and FBG Sensor Layouts

Large differences of environment temperature between winter and summer required the installation of two special fibres (transmitting and receiving) to ensure the accuracy of monitoring data (Zhang et al. 2014; Huntley et al. 2014b; Huntley et al. 2016). The BOTDR array to monitor the distributed strain in the sensor fibres was installed along the concrete retaining wall (**Figure 2b, c; Figure 3a, b**). Optical fibres were mounted to the retaining wall using double-sided adhesive and glue bonds every 1.5 m. An application of glue covering the whole optic fibre network prevented deformation loss during the curing process. Approximately 1000 m of fibre-optic cable was attached to the retaining wall, with another 1000 m fed under the CP tracks, through a buried conduit, and into the bungalow where it was connected to BOTDR

monitoring system (Figure 2d). Vertical and horizontal FBG strain and displacement sensors were installed approximately 50 m from the southwest end of the retaining wall in the vicinity of GPS 3, where sagging of lock-blocks was evident (**Figure 3a**). Strain (and displacement) was monitored within the retaining wall in the vicinity of GPS 3 by positioning FBG displacement sensors vertically and horizontally across individual locking blocks. In the CP bungalow, BOTDR and FBG monitoring instrumentation, the computer server and power converter were connected through RS232 cables (**Figure 2a**). Software installed on the server included Microsoft SQLServer2005TM, Tomcat6TM and a data monitoring software platform (**Table 1**). When functional, the server connected to the internet network through a wireless modem allowing access to real-time to monitoring data.

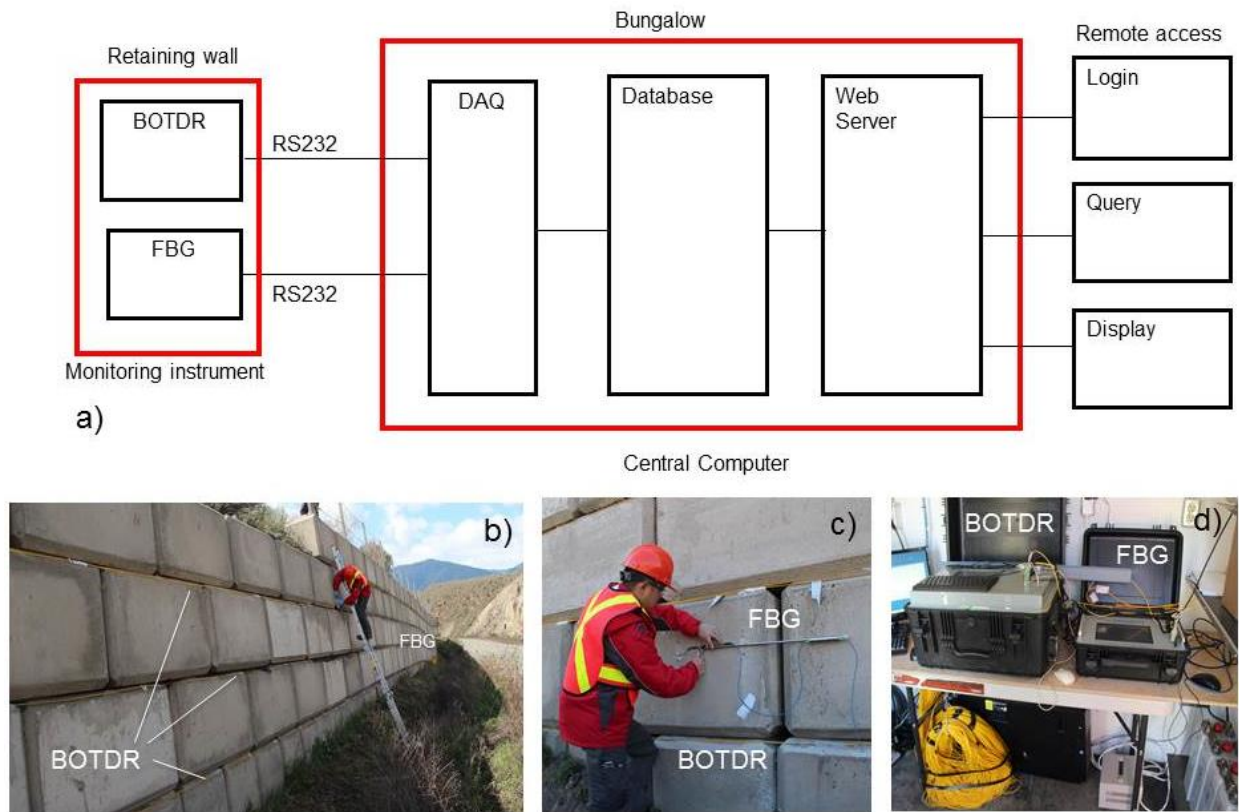


Figure 2 a) Schematic design of the optical fibre real-time landslide monitoring system, combining BOTDR, FBG, databases and web server technology; b) installation of fibre-optic cables for BOTDR along lock-block retaining wall; c) installation of FBG sensors – horizontal displacement rod attached to adjacent concrete blocks; d) monitoring computing area – CP bungalow.

Operating System	Windows Server 2008	
Application Software	Microsoft SQLServer2005	Database software platform using integrated business intelligence (BI) tools and providing enterprise data management
	Tomcat6	Web server software with the advantage of static pages that can handle a large number of network customer requests
	Jdk1.6	The Java developer kit contains the basic Java language development tools provided by SUN company
	Datacollection.exe	Independently developed application software (CHEGS) that functions to receive data transmitted from BOTDR and FBG instruments through RS232
	Data monitoring platform	Independently developed application software (CHEGS) that functions to manage monitoring data from BOTDR and FBG instruments, accessed on site or remotely through the network remote login and data query packages

Table 1 Software installed in the server located in the CP bungalow.

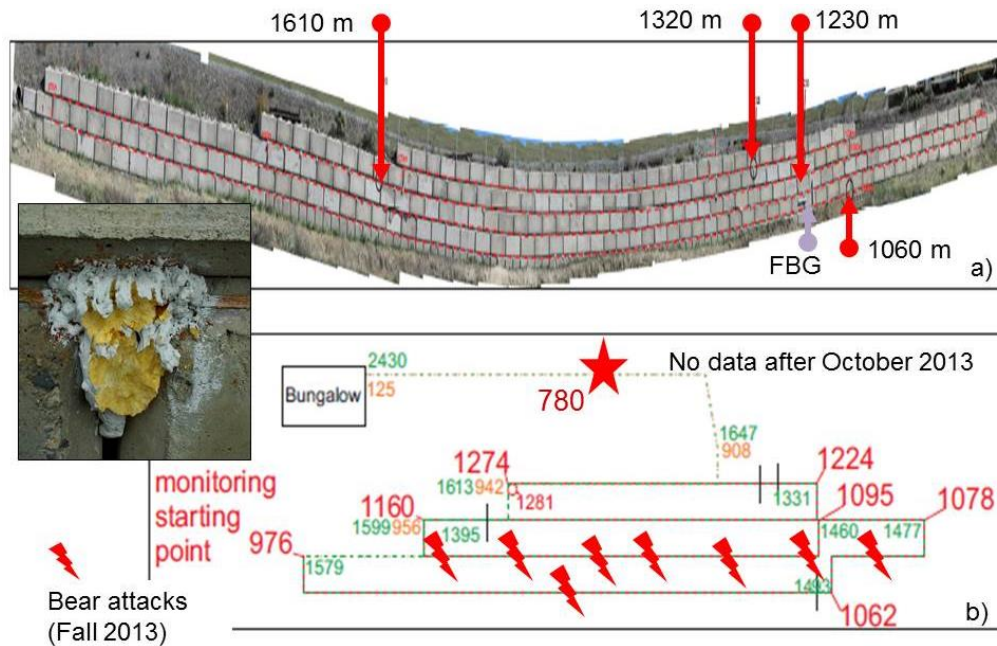


Figure 3 BODTR and FBG monitoring arrays: a) Installation network on retaining wall along shown as thin red line, also indicated are locations where obvious strain detected prior to failure in October 2013; b) Plan of installation and connection to monitoring instrumentation in CP bungalow, showing where fibre cables were damaged by a Grizzly Bear, and location of cable break formed in October 2013 that terminated the BODTR monitoring experiment.

3.4 Initial Operational Procedures for FBG and BODTR systems

Upon entering the bungalow, the first operational step was to check whether the BOTDR instrument, FBG instrument and modem were connected to the power supply and to the Internet (**Figure 4**). The next step was to check if the blue network cable was connected to the computer (server), and whether the lights were flashing to indicate a connection cable (**Figure 5**). To confirm whether the computer could connect to the Internet, *Internet Explorer* was opened on the monitoring computer server and <http://www.ip138.com> was input in browser window. When successfully connected, the link shown in **Figure 6** opened.

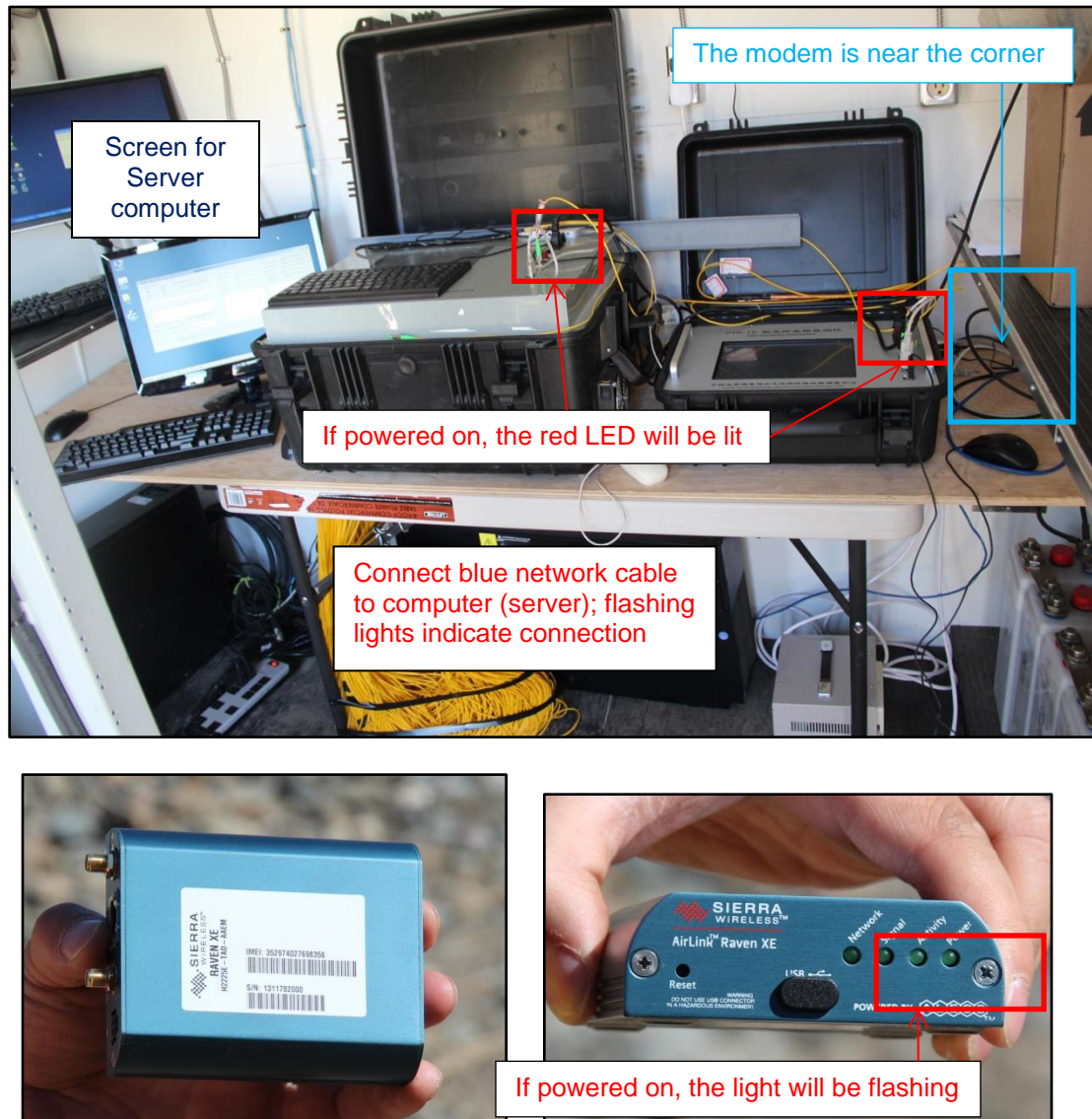


Figure 4 Key components to the FBG and BODTR monitoring systems housed in the CP bungalow.

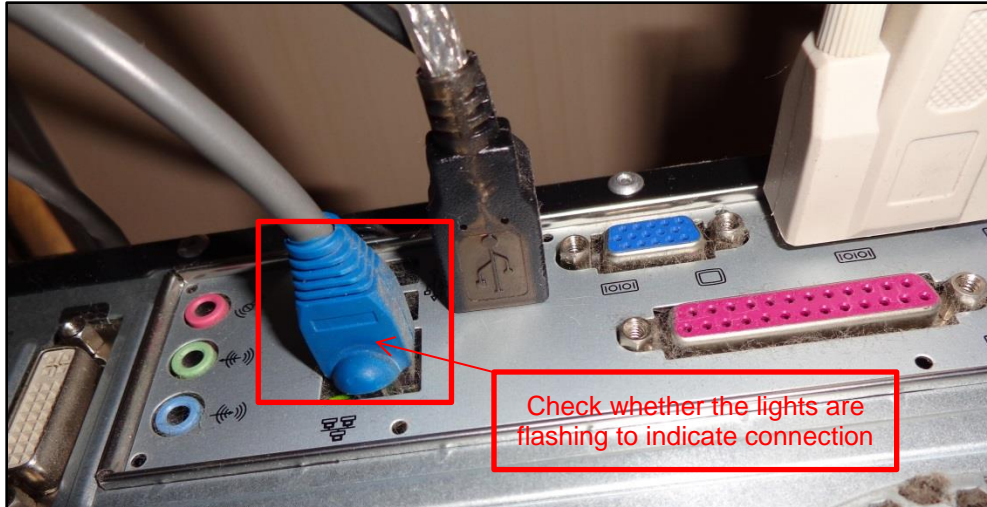


Figure 5 Correctly installed network cable at the back of the computer server.



Figure 6 Screen shot of monitoring software for FBG and BODTR.

4. Optical Fibre Bragg Grating Monitoring Demodulation (FBG) Device

Optical fibre Bragg grating monitoring demodulation (FBG) devices (**Figure 7a, b**) are used for high precision, high resolution, multi-purpose monitoring. The average refractive index of the fibre grating and grating cycle are sensitive to environmental parameters. Fibre grating demodulation devices convert changes in environmental parameters into a shift of the Bragg wavelength. Environmental parameters are demodulated through the shift of Bragg wavelength. FBG devices are mainly installed to measure structure body temperatures, strain, monitoring displacement in bridges, tunnels, slopes, architectures, dams and active landslides; in addition, there are other, health monitoring applications.

4.1 Technical specifications

The main technical specifications of optical fibre grating monitoring demodulation devices used at the Ripley Landslide test site were as follows:

- 1) Channels – 1CH (Channels expandable)
- 2) Each channel connected to a maximum number of 40 FBG sensors. The number of channels connected was related to the sensor measuring range. When measuring with a wide sensor range, fewer channels were used to avoid measuring wavelength overlap (interference).
- 3) Tuning Range 1525~1565nm
- 4) Wavelength Demodulation Accuracy ± 5 pm
- 5) Dynamic Range >50 dB
- 6) Sweep Speed 200Hz
- 7) Optical Connector FC/APC
- 8) Power Supply AC 220V, DC 12V

Before measurement, the adapter connector of the optical fibre sensor was cleaned with an alcohol sponge. After waiting for the alcohol to completely evaporate, the adapter connector was connected to the optical interface connector on the front panel. Once the measurement was completed, protection caps were placed on the optical interface connector to prevent the entry of dust. A quick view guideline to operating the FBG system is presented in Appendix 2.

4.2 Operating FBG Modulation Software


The “**Start Interface**” used to select the working mode and exit the system (**Figure 7c**) was accessed by the following steps.



Figure 7 a) Fibre Bragg grating demodulation unit similar to that installed at the Ripley Landslide site; b) front panel; (1) LCD screen touch screen display or human-machine interface, (2) FUSE (note, unit at Ripley Landslide also has an Antenna Port), (3) 12V input, (4) Power LED, (5) Power Switch, (6) Optical interface connector, (7) RS-232 interface connector, (8) USB interface connector (not on the unit at the Ripley Landslide); c) Start Interface.

1) Clicking the “**Manual Mode**” button  entered the manual measurement interface.

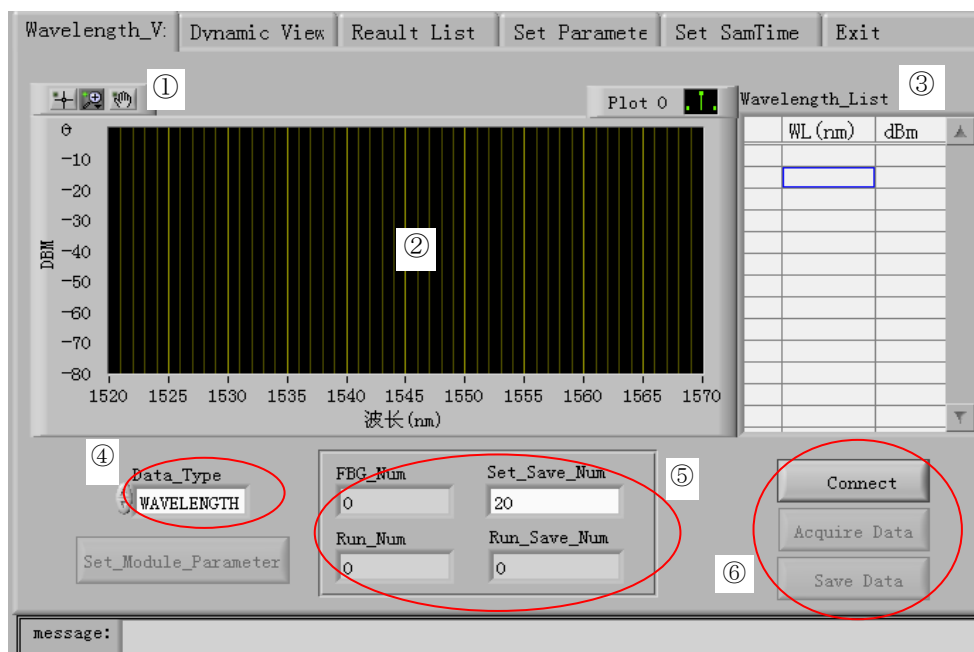
2) Clicking the “**Automatic Mode**” button  entered the automatic measurement interface.

3) Clicking the “**STOP**” button  when the measurement finished exited the FBG grating data acquisition system.

4) **Power off** when 可以关闭电源了 showed.

4.3 Manual Measurement Mode

Figure 8 shows the on-screen display of the monitoring data chart and data sheet for the Wavelength Acquisition Interface.



- ① Option Button
- ② Monitoring Data Chart
- ③ Monitoring Data Sheet
- ④ Acquisition Data Type
- ⑤ Acquisition Parameter
- ⑥ Function Keys

Figure 8 Wavelength Acquisition View

The Wave Acquisition View was accessed using the following steps:

1) Clicking the “**Test Connection**” button  performed a self-test that took approximately 1-2 seconds to execute.

2) If the self-test was successful, “**The FBGA is connect**” was displayed in the "message" box.

3) If the self-test failed, “**The FBGA is error !**” was displayed and a prompted was sent to check connections.

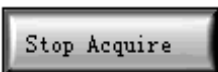
4) The button  selected the type of acquisition data.

5) Selecting the “**VOLT**” acquired the amplitude data of the spectrum; X coordinate of the chart, wavelength range; and Y coordinate, the spectrum amplitude; amplitude spectrum data was displayed in the data list.

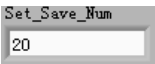
6) Select the “**DBM**” acquired the power data of the spectrum; X coordinate of the chart is wavelength range; Y coordinate is the spectrum power; the power spectrum data is displayed in the data list.


7) Select the “**WAVELENGTH**” acquired the wavelength data of sensors; X coordinate of the chart is wavelength range; Y coordinate is the wavelength of sensors; wavelength data is displayed in the data list.

8) If the self-test was successful, the “**Began Analysis**” button  was clicked.

9) If data was being acquired, the button became  and data was displayed in the chart and data list.

10) Clicking the “**Wavelength Display Stop**” button  restored the button .

11) Entering “**Save-number**”  saved the acquisition data.

12) Clicking the “**Save data**” button  saved the file dialog displayed in **Figure 9**.

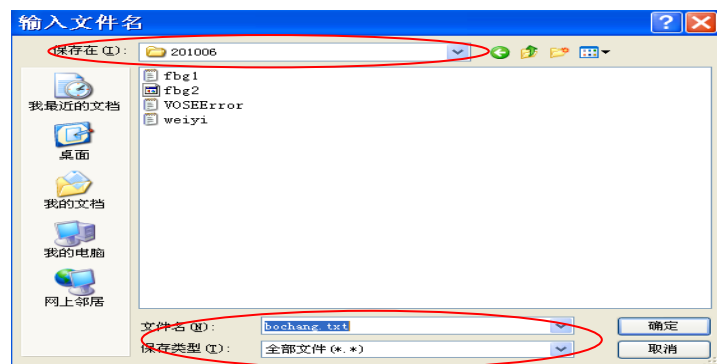

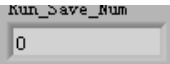


Figure 9 Save file dialog.

13) A filename was entered and the file type selected, then the button  was clicked to save the acquisition data as the file.

14) “**Executive save number**” was shown in .

15) When reached the save stopped.

16) The number of sensors was then shown:

4.4 Dynamic Interface

Figure 10 is a view of the interface showing the dynamic display of wavelength data of the FBG sensors.

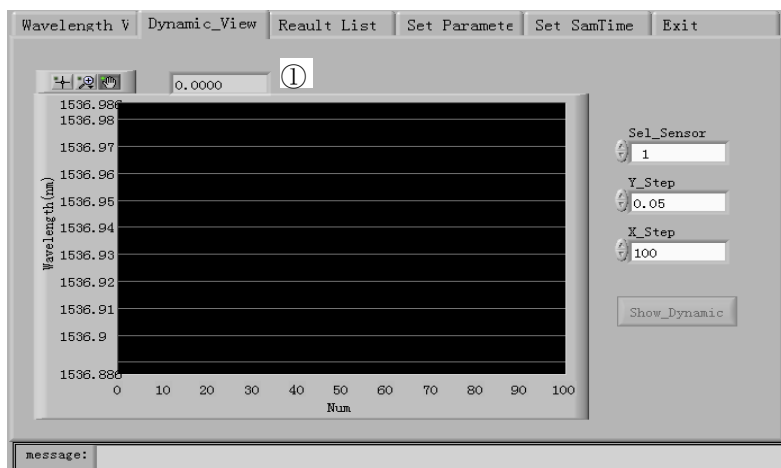


Figure 10 Dynamic interface view: 1 - current testing wavelength.

1) The “**Sensor number**” was shown in ; the arrow of textbox was used to change the number of the sensor.

2) Clicking the button displayed the wavelength of the selected sensor in the chart; clicking the button again stopped the display.

3) The arrow of textbox changed the Y range.

4) The arrow of textbox changed the X range.

4.5 Set Parameters Interface

Figure 11 shows the interface for setting each sensor parameter.

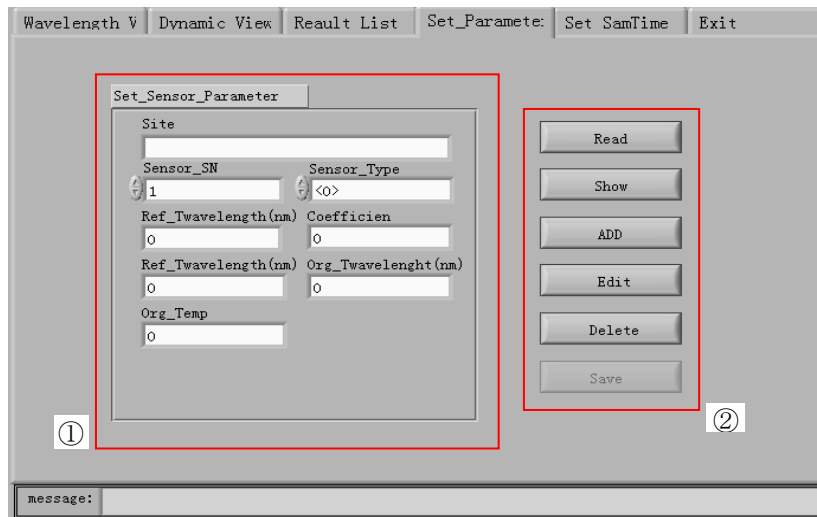


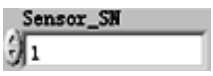
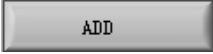

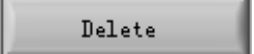

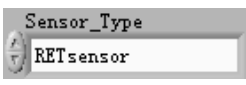


Figure 11 Set Parameters interface: 1) Parameter Settings Area; 2) Function Keys.

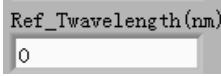
To calculate the sensor measuring results, parameters of the sensor were set according to the type of sensor.

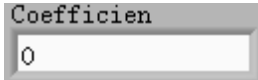
- 1) If sensor parameters were set and stored, click  opened the file.
- 2) If the parameters were not set, they had to be set the parameters using the parameter setting area.
- 3) Clicking the  button displayed the sensor parameters.
- 4) Clicking the left arrow button  changed the number of the sensor to check; parameters of this sensor were displayed in these textboxes.
- 5) To add, modify and delete these sensor parameters, the ,  or  were buttons; operation results were shown in the message textbox.
- 6) Clicking the  button saved sensor parameters as a file.
- 7) Clicking on the left arrow button  selected the type of sensor

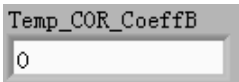
The types of the sensors available were as follows:

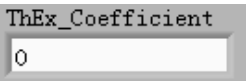
TCS sensor (used on the Ripley Landslide)

The *fibre Bragg grating strain sensor* with the temperature correction required the setting of parameters such as:

a) Reference strain wavelength 

b) Strain coefficient 

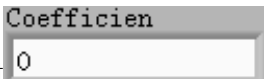
c) Temperature correction coefficient 

d) Coefficient of thermal expansion 

SFS sensor

The *surface fixed fibre Bragg grating strain sensor* was designed to be mounted on an object needing to be monitored. The wavelength was measured, but this measurement was not influenced by external conditions. Since this type of sensor was without the temperature compensation grating, an external temperature sensor was needed to correct for the influence of temperature on strain. The surface fixed fibre Bragg grating strain sensor required the setting of parameters, such as:

a) Reference strain wavelength 

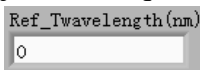
b) Strain coefficient 

EMS sensor

An *embedded fibre Bragg grating strain sensor* required the same parameter settings as the SFS sensor.

RET sensor

A *reference temperature fibre grating sensor* measured the reference temperature wavelength in a sensor mounted on the monitored object and required the setting of parameters such as:

a) Reference temperature wavelength 

- b) Temperature coefficient A
- c) Temperature coefficient B
- d) Temperature coefficient C
- e) Original temperature wavelength
- f) Original temperature

SFY sensor

The *fibre Bragg grating reinforced force measuring sensor* required the setting of parameters such as:

- a) Reference strain wavelength
- b) Strain coefficient

NAK sensor

The *bare grating sensor* required the same parameter settings as the SFY sensor.

TCP sensor

The *fibre Bragg grating strain sensor grating with temperature compensation* required the setting of parameters such as:

- a) Reference strain wavelength
- b) Strain coefficient
- c) Reference temperature wavelength
- d) Temperature correction coefficient
- e) Original temperature wavelength
- f) Original temperature

g) Coefficient of thermal expansion

DIS sensor

This *fibre Bragg grating displacement sensor* required the setting of parameters such as:

a) Reference displacement wavelength

b) Displacement coefficient

c) Reference temperature wavelength

d) Original temperature wavelength

e) Original temperature

TMP sensor

This *temperature fibre grating sensor* required the setting of parameters as the RET sensor.

SYJ sensor

The *fibre Bragg grating seepage pressure sensor* required the setting of parameters such as:

a) Pressure reference wavelengths

b) Pressure coefficient

c) Reference temperature wavelength

d) Temperature correction coefficient

e) Temperature coefficient

f) Original temperature wavelength

g) Original temperature

h) Coefficient of thermal expansion

4.6 Test Results Interface

Test results were accessed through the operational steps outlined in this section. Test results were displayed in the interface shown in **Figure 12**.

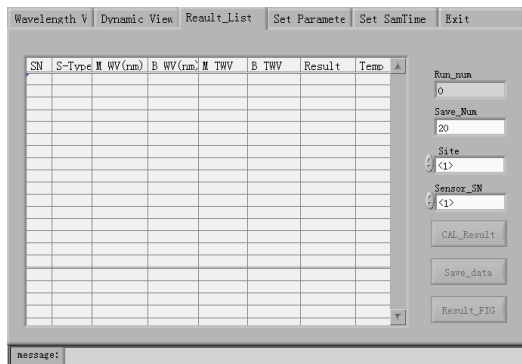
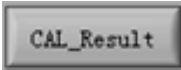



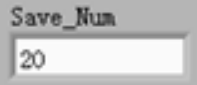
Figure 12 Test Results view interface.

- 1) Clicking the button 
- 2) Button turned to 

The measured result of the sensors was counted and resultant data displayed in the data list.

- 3) Clicking the button again and stopped the calculation.

If the sensor did not have temperature-compensating grating, the *temperature measuring wavelength*, the *reference temperature wavelength* and *temperature* were **0**. The *current measuring wavelength* and the test results was the same as the sensor type.

- 4) To save the test results, the number of saves was set in the textbox 

- 5) Clicking on  saved test results as a file.

- 6) When  equaled 

- 7) Clicking the button  automatically returned to the default state.

- 8) If the number of saves was not set, the default number was 20.

- 9) Clicking on the left arrow  changed the sensor number to be checked.

- 10) Clicking the  button.

- 11) Turned on 

The measured result was dynamically displayed in the test chart. If the sensor had the temperature compensation grating, then the measured temperature result was dynamically displayed in the temperature chart at the same time (as was the case for the Ripley Landslide installation).

12) Clicking again  closed the measured results chart.

4.7 Acquisition Time Setting Interface

Figure 13 shows the settings of automatic acquisition time and acquisition interval.

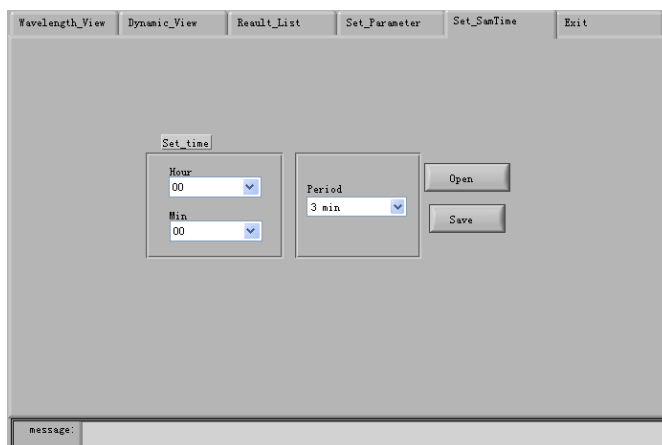
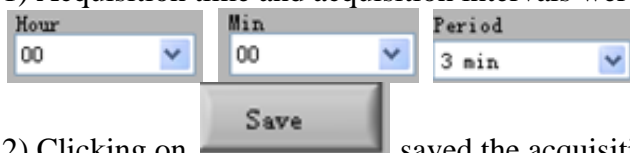
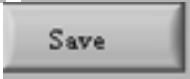


Figure 13 Acquisition Time Setting view.

1) Acquisition time and acquisition intervals were set using following buttons:



2) Clicking on  saved the acquisition time and acquisition interval. The filename was [D:\FBG\timing.txt](#)

3) Clicking on  opened a saved file.

4) The acquisition time and acquisition interval were read from the document and displayed respectively in:



4.8 Exit View

This page (**Figure 14**) allowed the user to safely exit the software by following the steps below.

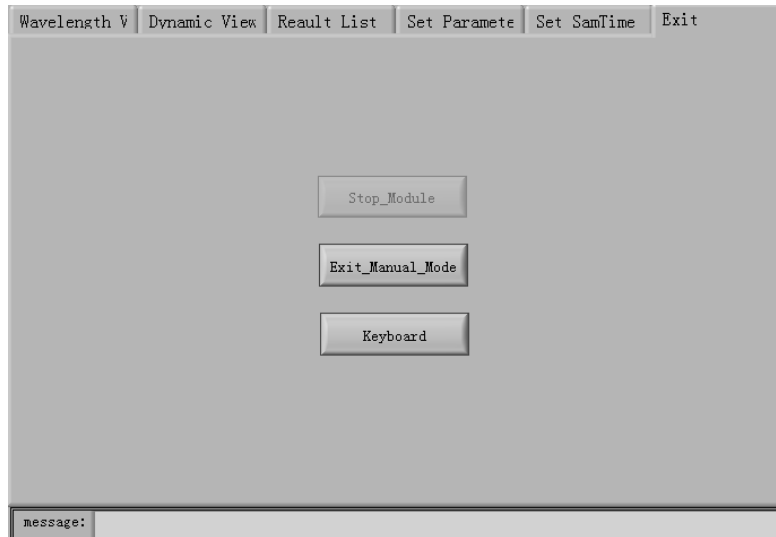


Figure 14 Exit Manual Mode view.

1) Clicking on "**Stop the demodulation module**"  exited the demodulation module in manual mode.

2) Clicking on "**Quit the artificial measurement mode**"  changed the view from manual mode to the main interface.


3) Clicking on "**Soft keyboard**"  opened a soft keyboard; data and characters could then be entered on screen (**Figure 15**).



Figure 15 Soft keyboard

4.9 Automatic Measurement Mode

In the automatic mode (**Figure 16**), acquisition time and acquisition interval were acquired automatically by the device. When the acquisition time was reached, the system was activated automatically, with power supplied to each module. The optical fibre grating monitoring demodulation software was run and measurement data were saved and transmitted through the

wireless transmission module. After measurement, if the acquisition interval time was more than 1 hour, the system shut down power to each module and entered a dormant state until the next acquisition time. If the acquisition interval time was less than 1 hour, the system was delayed until the next acquisition time.

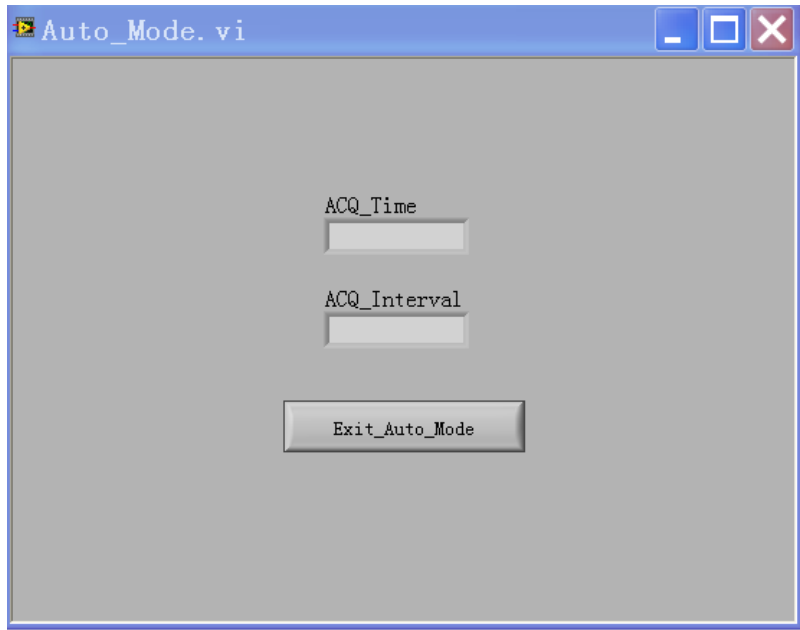


Figure 16 The automatic measurement mode.

1) Acquisition parameters were entered in the buttons:



2) “**Exit the automatic measurement mode**”  was then clicked.

3) The screen view changed from the *automatic measurement mode* to the *main interface*.

5. Distributed Fibre Optic Strain (BOTDR) Monitoring System

The distributed fibre optic strain, or Brillouin Optical Time Domain Reflectometry (BOTDR) monitoring system integrated data acquisition and storage processes. There was a control circuit so that instrument ran automatically when the acquisition time was set. The system was equipped with a high-end computer: an important part of the instrument that controlled the whole system, collected and stored data, ran the real-time display, and effected transmission of data. To make operation easier for the user, the computer's universal interface was retained. **Figure 17** shows an instrument similar to that installed at the Ripley Landslide site. The system contained software for both data acquisition and data transmission (**Table 2**). The host configuration included a keyboard, mouse, power line, network cable and serial line. Also included were backup software CD and an operating manual. Technical features of the instrument acquisition system included: a maximum optical fibre length of 30 km; a temperature sensing accuracy of $\pm 1^{\circ}\text{C}$; a strain sensing accuracy of $100\ \mu\epsilon$; and a spatial resolution $< 5\ \text{m}$. For display and recording the following was used: Intel Atom D510/D525, 1.66 / 1.8GHz CPU host processor with 1GB of RAM, a built-in 32GB hard disk, a 800×600 10 VGA display; standard USB and serial port 232 connectors; and strain file and original data (.txt) record file formats; and a Windows 2000 operating system. The host size was $613 \times 488 \times 406\ \text{mm}$, and power consumption varied from 9.46W on standby to 180.4 W during data acquisition.

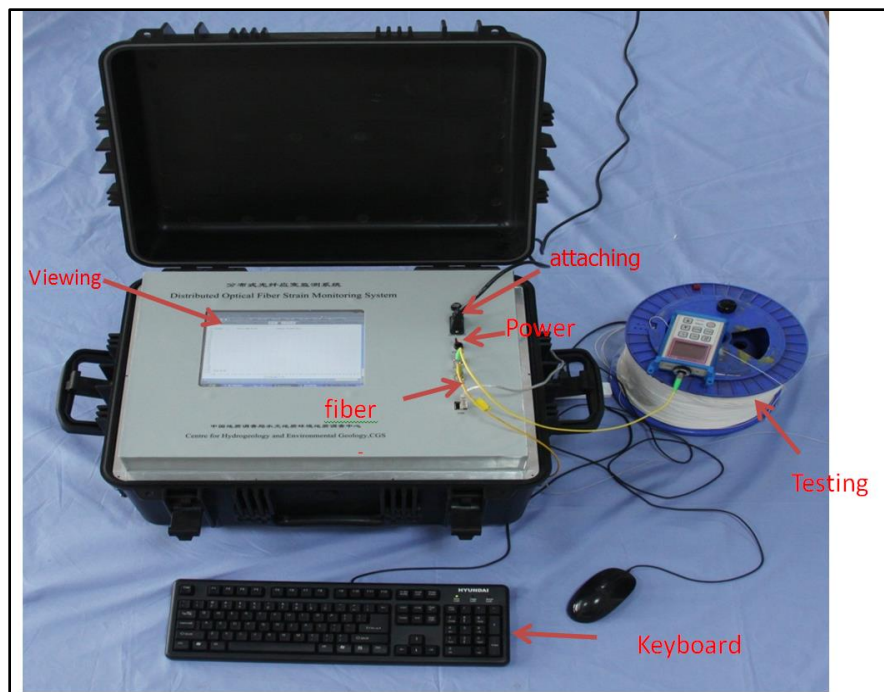


Figure 17 Key elements of BOTDR instrument.

Environment requirements restricted the operation of this system. Fierce vibration was avoided during transport to prevent loss of internal screws or damage to computer hard disk. The optimal safe operating temperature range was 0°C to 40°C , with an optimal temperature of 20°C . These

temperature extremes were exceeded in the Thompson River valley a number of times between 2013 and 2016. The operation of this instrument during periods of rapid temperature change was counter-indicated. Also critical to the monitoring process was the need to maintain a clean optical fibre external interface. Dust, a common issue at the Ripley Landslide site, resulted in optical signal attenuation and affected the quality of data collected. Appendix 3 outlines a quick view for operating the BOTDR system.

5.1 Acquisition software interface and acquisition process

While hooking up all power lines, the serial line and network cable between BOTDR and the server were also connected. Next, the server was opened to execute the MyQQ.exe application programs. The BOTDR unit was started by powering on the system. The unit remained on standby until acquisition time was set. After collection, data was transmitted to the server. Relevant strain data was downloaded for analysis by remote access from the server website. **Figure 18** shows a sweep frequency image that displays all signal amplitude images from setting lowest frequency to highest. A scanning amplitude curve at a certain frequency (10.440 GHz); the *abscissa* was the fibre length (unit: km) and the *ordinate* was the voltage amplitude (unit: mV) as shown in **Figure 19**. For the strain curve shown in Figure 20, the abscissa was the fibre length (unit: km) and the ordinate is strain value (unit: 100 $\mu\epsilon$).

Name	Instruction
app. exe	Acquisition software program
MyQQ.exe	Data send and acceptance program
RefFreqdata_32KM.txt	Frequency reference file (stored in the C-drive data folder)
ezusbw2k.inf	Driver file
ezusbpro.sys	
monitorcar.sys	

Table 2 System software and drives.

After collecting data over 20 time intervals, the software saved a strain file and sent it to the server. At this time, “Data is Sending” was displayed until data transfer finished. The display then went to the next time data collection interval, 10 times later, saved a file, sent it to the server, entered into next time, 5 times later, saved a file and again sent it to the server.

Meanwhile, an original data file was also saved on the instrument's built-in computer hard disk. This file was sent to the server by data transmission software.

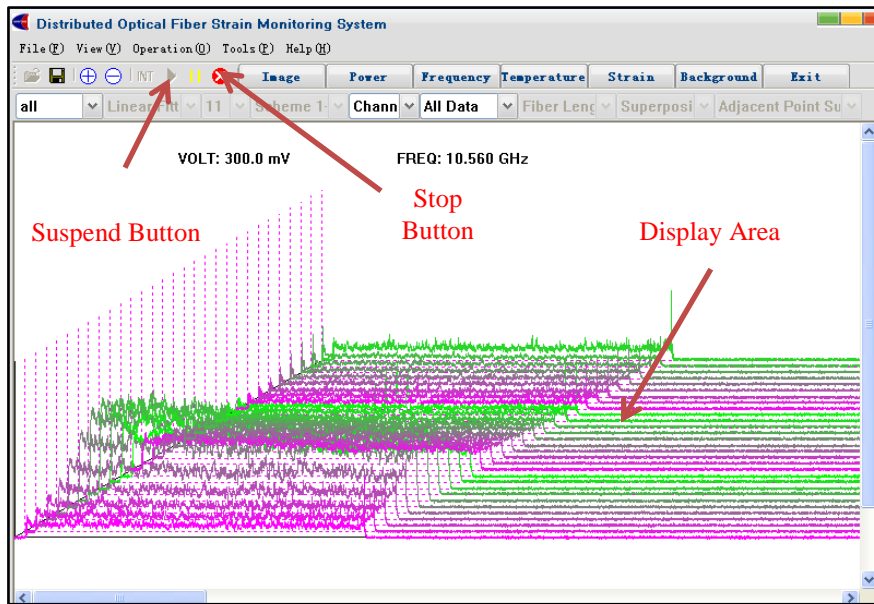


Figure 18 Frequency image at 10.560 GHz.

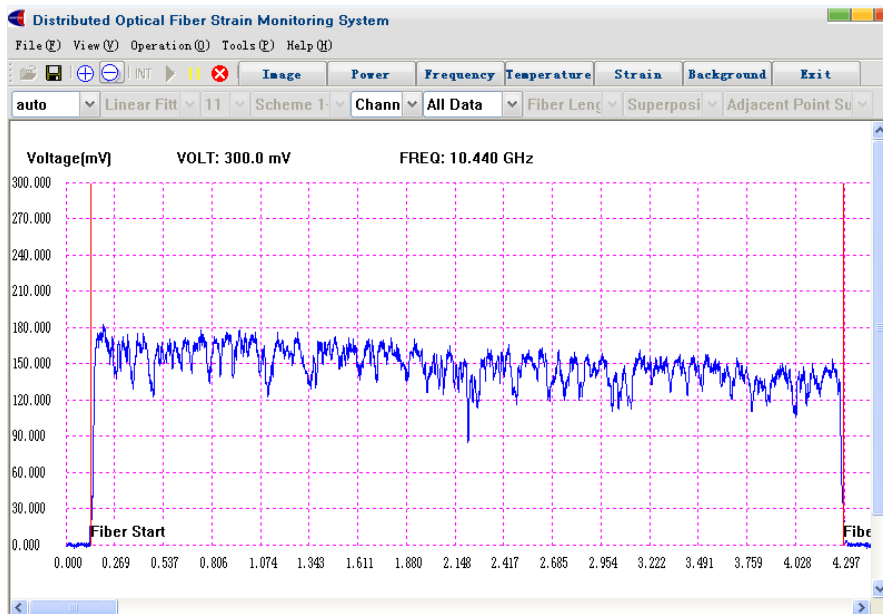


Figure 19 Scanning amplitude curve.

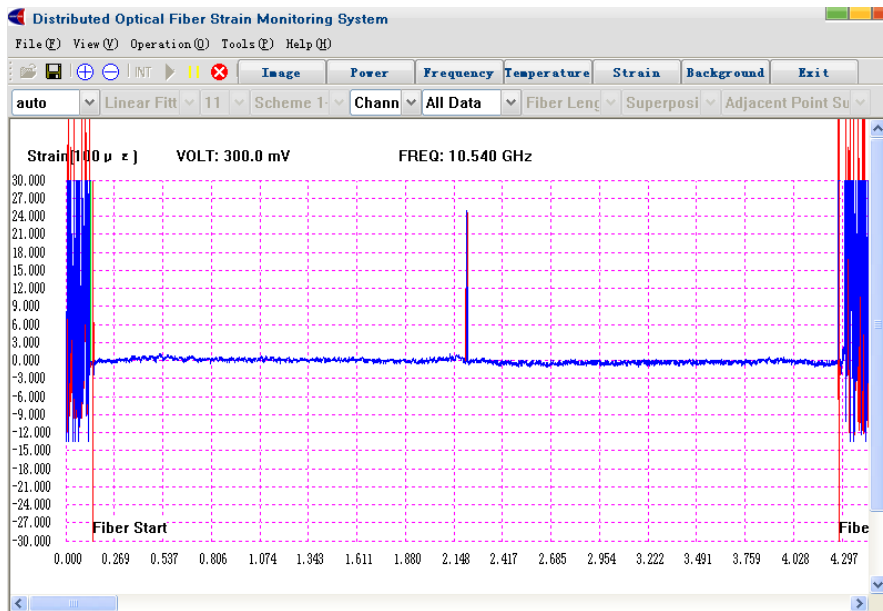


Figure 20 Strain curve.

5.2 System data receiving software

The main function of this software was to receive strain file documents and the original data transmitted by acquisition instrument, and to save it on the server. In addition, the software also saved a file path under the serial number setting. **Figure 21** shows the software interface.

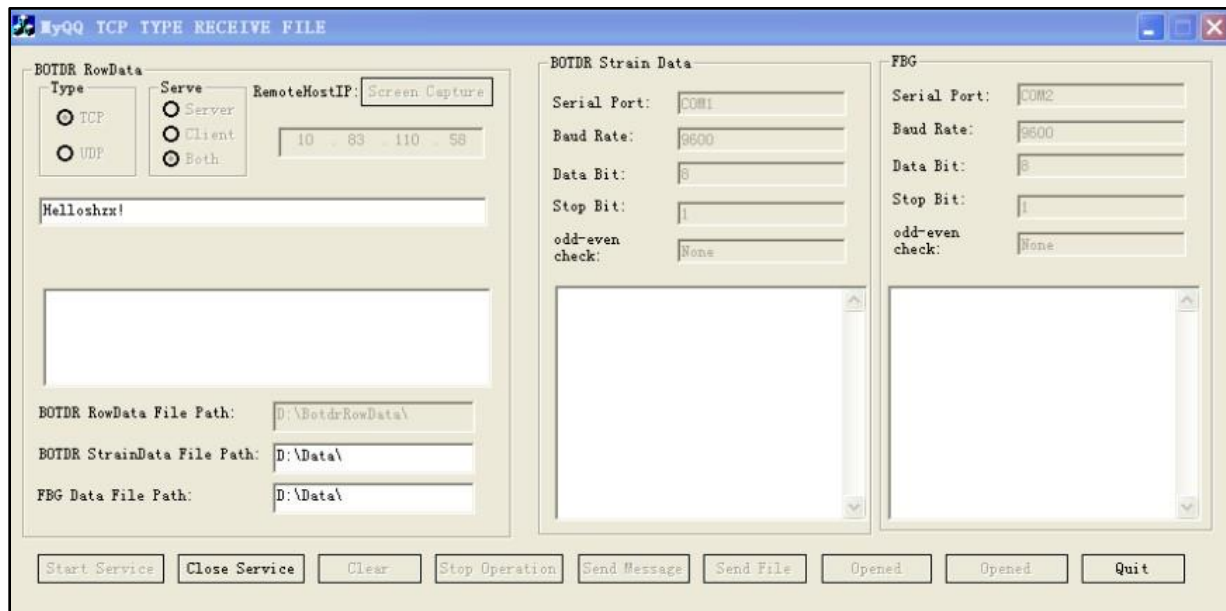


Figure 21 Software interface.

6. Data Monitoring Platform

6.1 Logging into the monitoring platform

When opening the software, a login page (**Figure 22**) first appeared. To enter the data monitoring system, the following were input "User Name", "Password" and the correct **Verification Code**. Once entered, the "Login" button was clicked. For convenience, on the next login, the user could choose to remember the current username and password. When user logged into the system (**Figure 23**), an authorization management function module required user functional and data authorization. According to the control of permission privileges, users could access authorized resources to prevent others from modifying system data and to improve system data security.

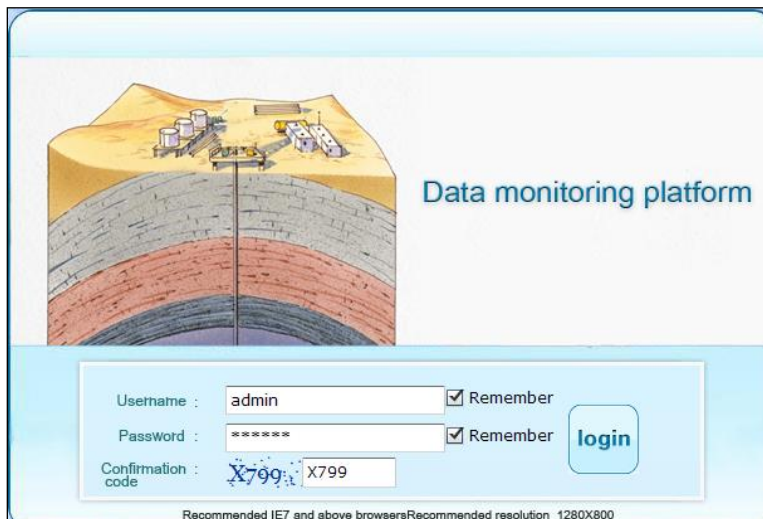


Figure 22 Login page.

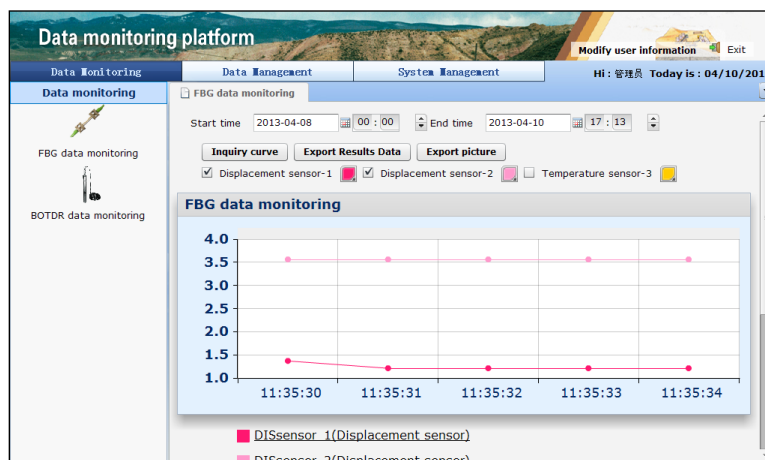


Figure 23 System home page.

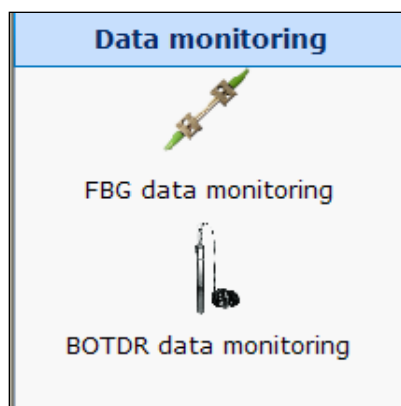


Figure 24 Monitoring data types.

Depending on the function authorized content, the platform system automatically generated some function modules that could be operated by current user such as **Control**, **View**, **Modify**, and other functions. Depending on the access authorization, the platform system automatically displayed the monitoring data, including FBG and BOTDR monitoring data viewed by current user (**Figures 23** and **24**). It also displayed the monitoring data in the form of a linear graph, which was more convenient for data analysis (**Figure 25**).

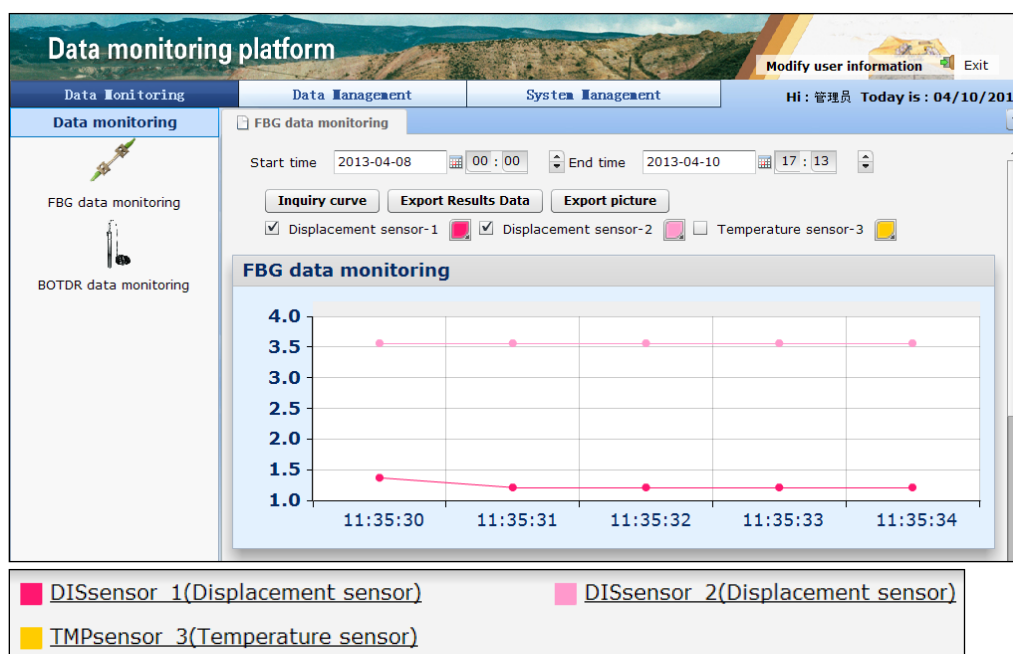


Figure 25 Monitoring data.

6.2 FBG data monitoring

This module displayed the FBG monitoring data in the form of a linear graph, which was more convenient for data analysis (**Figure 26**). The user could change the colour of each curve (to match a colouring convention) by clicking the colour configuration tool after the colour label (**Figure 27**).

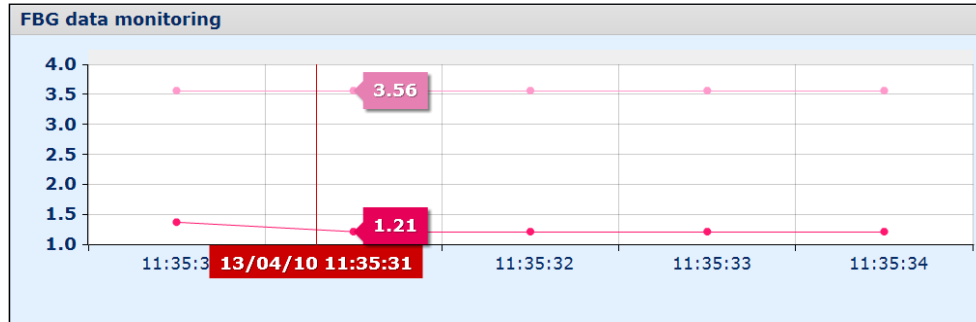


Figure 26 FBG data monitoring.

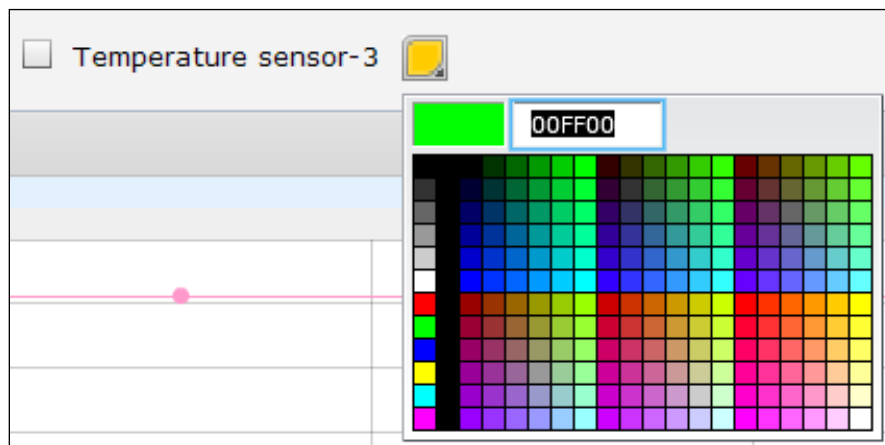


Figure 27 Colouring data points and curves.

The user was able to query monitoring data by setting time limit. This involved selecting the correct "start time" and "end time" in the "time selection" box, and then clicking the "Inquiry curve" button to display all the sensor data curves during the selected time in FBG data monitoring diagram. For the convenience of the user's query operation, the platform system provided a function of precise query. The user pressed the left mouse button, dragged then released the mouse after selecting the data area; the monitoring data curve within the selected data area could then be viewed (**Figure 28**).

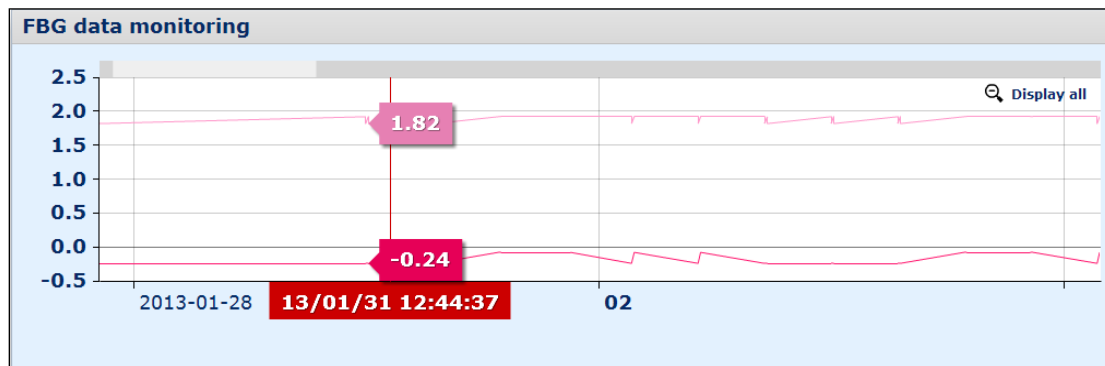
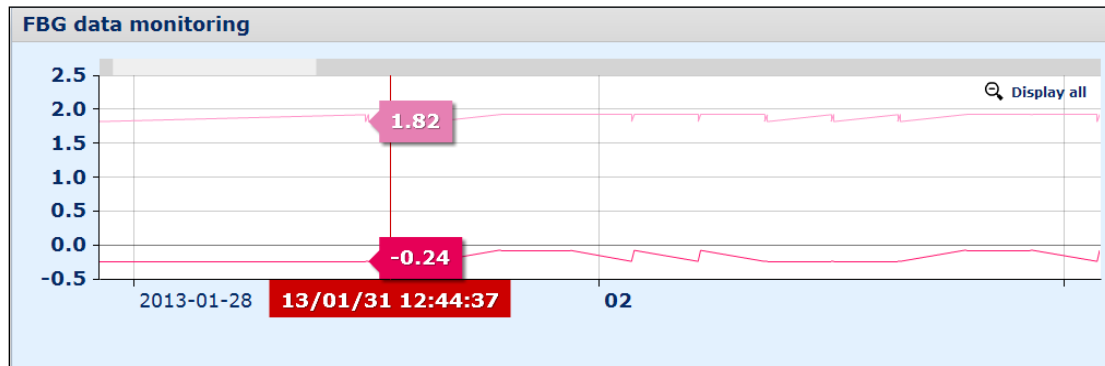
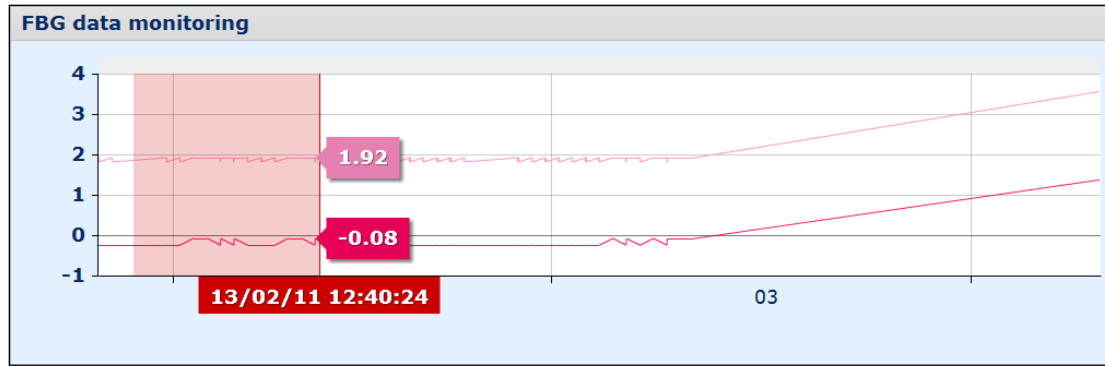


Figure 28 FBG data monitoring.

If the user wanted to view the all FBG monitoring data, the "**Display all**" button in the top right corner was clicked. The platform system provided legends below the line graph (**Figure 29**), and each data monitoring curve corresponded to a legend. When the query curve was too large, the user could click the legend to hide the monitoring curve corresponding to the legend and the legend icon greyed out. The data curve was made visible again when clicking the sensor legend again. For the convenience of the user to analysis data, the platform system provided a function of data contrast analysis base on the monitoring time, and the user was able to choose different sensors and different times for the display curve. Clicking the "**Add time**" button after selecting the monitoring point and time enable the user to see the monitoring time information added on the right side (**Figure 30**).

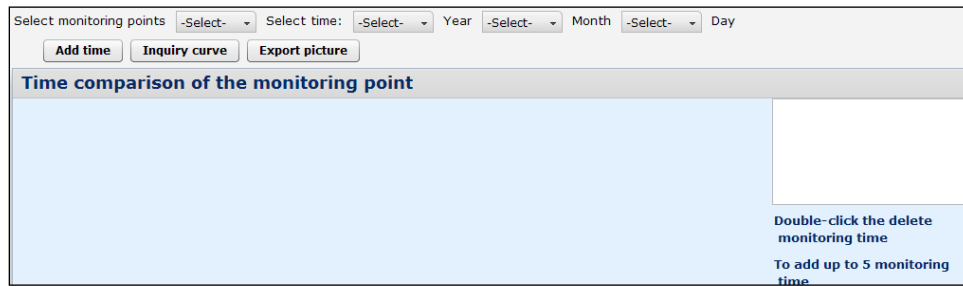


Figure 29 FBG data monitoring.

Clicking the “**Inquiry curve**” button generated the curve shown in **Figure 30**. Users could change the colour of the curve according to applied conventions. It should be noted that a maximum of 5 records could be added. When deleting a monitoring curve, double-clicking the “**Added monitoring time**” in the right side was necessary.

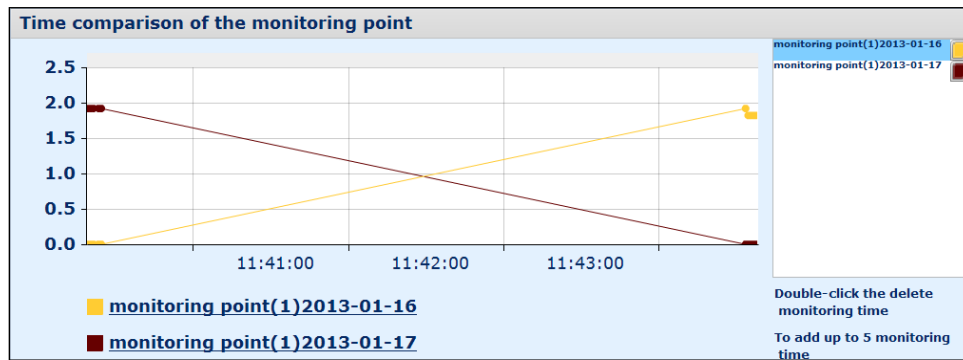


Figure 30 FBG data monitoring of linear graph.

This system provided an export function module to allow the export the result data for inspection of result data files. By clicking the “**Export Results Data**” button, a password confirmation dialog box popped up. The download password was provided in the user's personal information (**Figure 31**). Following the input the *password*, the “**Confirm**” button was clicked and a file download page popped up (**Figure 32**). Clicking the “**Download**” button enabled the user to download the file required (**Figures 32 and 33**).

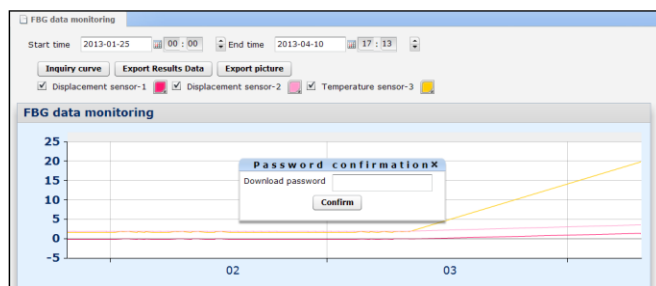


Figure 31 Password entry box.

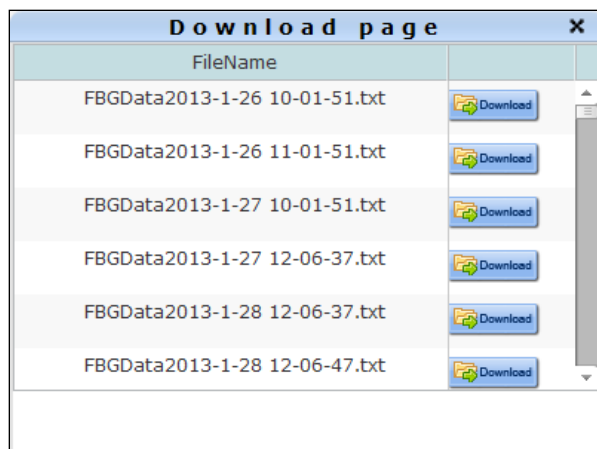


Figure 32 Download page.

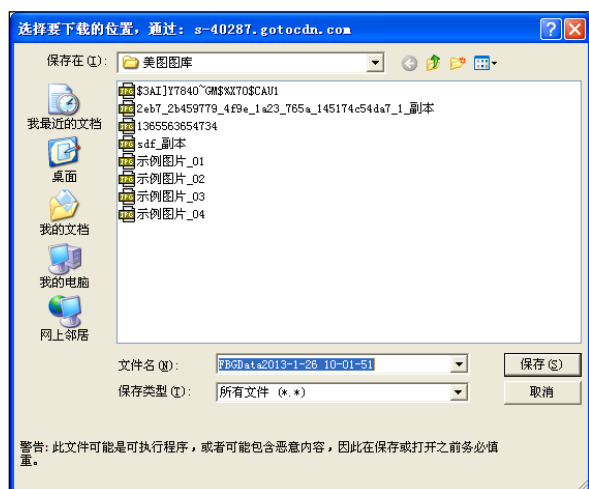


Figure 33 Save file and file type window.

6.3 BOTDR data monitoring

This module displayed BOTDR monitoring data in the form of a linear graph (**Figure 34**). The user could drag the mouse around to view individual BOTDR monitoring data values. Because BOTDR data volumes were much larger, all the monitoring points could be displayed in the figure; but it was also possible to view monitoring points that were not displayed by dragging the button (**Figure 35**). Clicking the “**Display all**” button returned the user to the initial data.

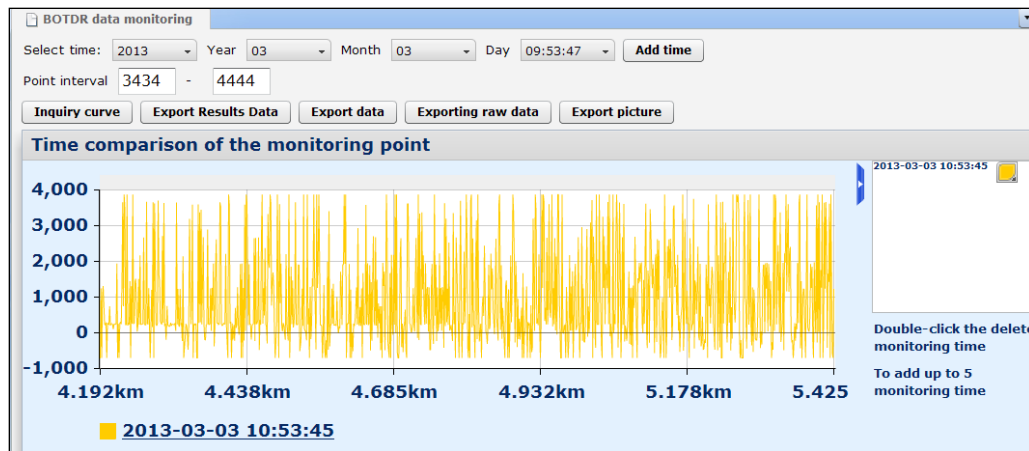


Figure 34 BOTDR data monitoring.

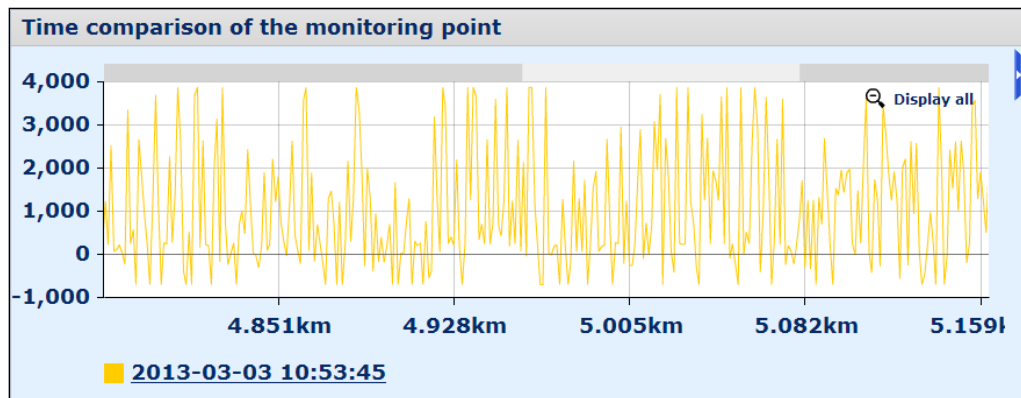


Figure 35 BOTDR data monitoring window in detail.

To select the year, month and day of the monitoring window, the “**Add time**” button was clicked to choose the monitoring data and the view range was input into the “**Point interval text**”. Clicking the “**Inquiry curve**” viewed the linear graph corresponding to the selected monitoring data (Figure 36). The user was able to change the colour of the curve according to applied conventions by clicking the colour configuration tool after the colour label (Figure 37). The BOTDR module also provided the function of downloading result data and original data. Clicking the “**Export Results Data**” button or the “**Export raw data**” button led to a password confirm dialog box popping up. Inputting the password and then clicking the “**Confirm**” button (Figure 38) enabled the download page to pop up. The user then clicked the “**Download**” button to download the file needed (Figures 39 and 40).

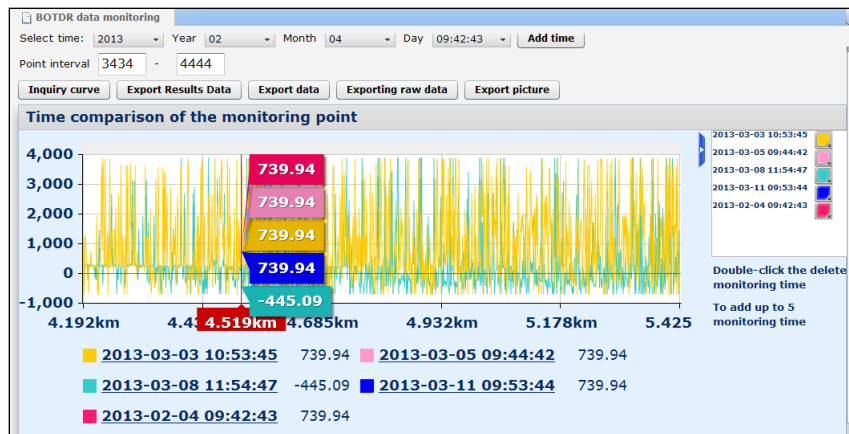


Figure 36 BOTDR data monitoring.

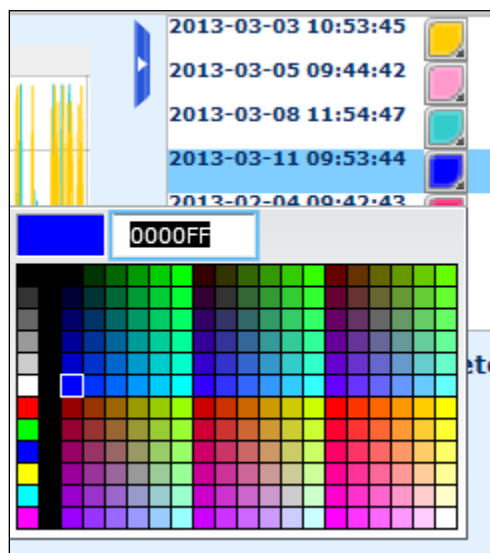


Figure 37 Colour configuration tool.

The dialog box is titled 'Password confirmation'. It contains a text input field labeled 'Download password' and a 'Confirm' button.

Figure 38 Password entry box.

Download page	
FileName	
BOTDRStrain2013-3-3 10-53-32.txt	
BOTDRStrain2013-3-3 10-53-45.txt	
BOTDRStrain2013-3-3 9-53-47.txt	
BOTDRStrain2013-3-5 9-44-42.txt	
BOTDRStrain2013-3-5 9-44-47.txt	

Figure 39 Download page.



Figure 40 Save file and file type window.

Since BOTDR monitoring data volumes were so large, no more than 8192 points were selected when viewing the BOTDR monitoring data (**Figure 41**). It was possible to select a length range of 1-10000 and add up to five curves. Because the large volumes of raw data volume, it took some time to export the raw data.

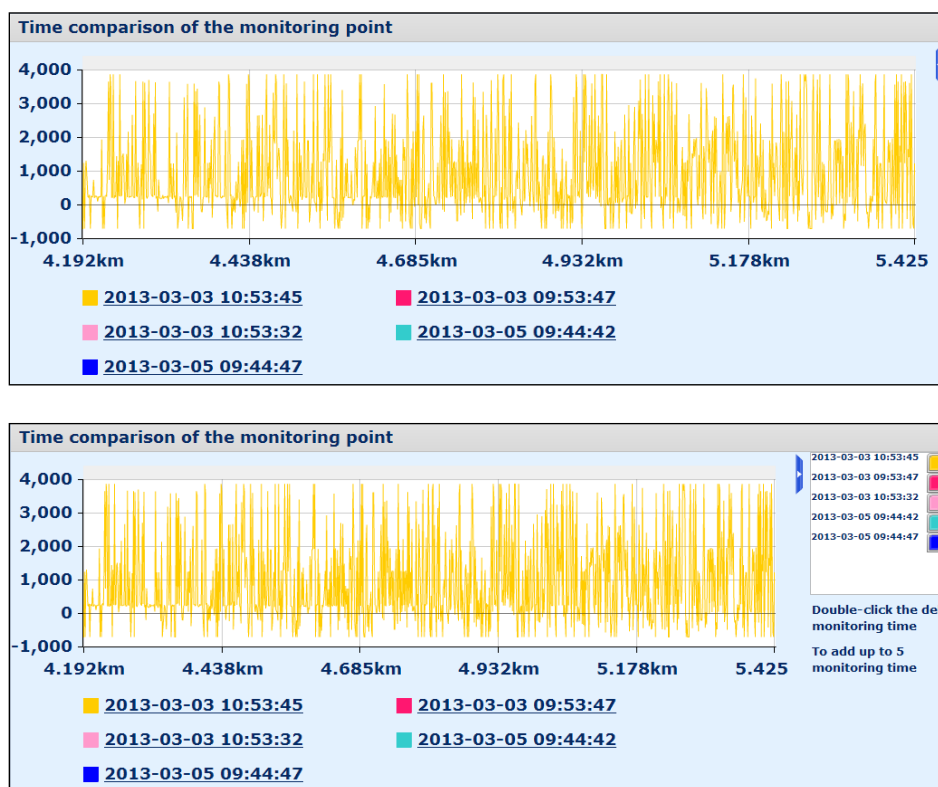
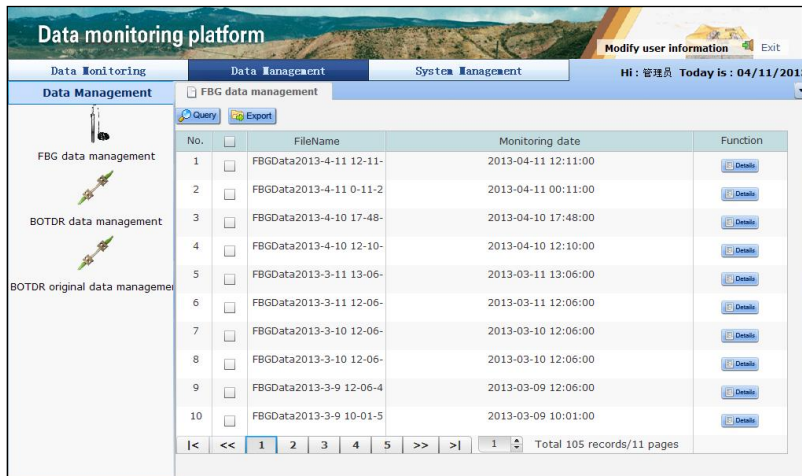


Figure 41 BOTDR data monitoring.

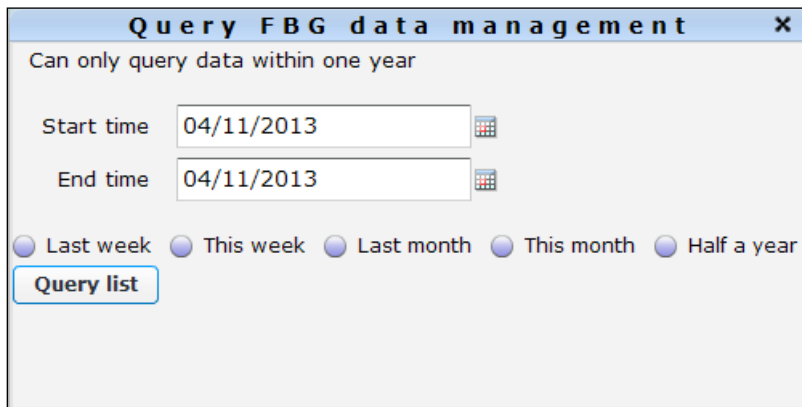
6.4 Data management

The platform system provided the function of monitoring data management maintenance (**Figure 42**). The three main operation instructions were: **Query**, **Export** and **View**. Clicking the “**Query**” button activated a pop up query window (**Figure 43**). The user then chose a query time then clicked the “**Query list**” button: a data list showing all data within this time period appeared (**Figure 44**). To export the data, the **Checkbox** was clicked along with a password input window pop up (**Figure 45**). After entering the correct password, the “OK” button was clicked (**Figure 46**). Files were saved in the file download window (**Figure 47**). Clicking the “**Detail**” button opened the view page (**Figure 48**).



No.	FileName	Monitoring date	Function
1	FBGData2013-4-11 12-11-	2013-04-11 12:11:00	Details
2	FBGData2013-4-11 0-11-2	2013-04-11 00:11:00	Details
3	FBGData2013-4-10 17-48-	2013-04-10 17:48:00	Details
4	FBGData2013-4-10 12-10-	2013-04-10 12:10:00	Details
5	FBGData2013-3-11 13-06-	2013-03-11 13:06:00	Details
6	FBGData2013-3-11 12-06-	2013-03-11 12:06:00	Details
7	FBGData2013-3-10 12-06-	2013-03-10 12:06:00	Details
8	FBGData2013-3-10 12-06-	2013-03-10 12:06:00	Details
9	FBGData2013-3-9 12-06-4	2013-03-09 12:06:00	Details
10	FBGData2013-3-9 10-01-5	2013-03-09 10:01:00	Details

Figure 42 Data management page with data management list.



Query FBG data management

Can only query data within one year

Start time: 04/11/2013

End time: 04/11/2013

☐ Last week ☐ This week ☐ Last month ☐ This month ☐ Half a year

[Query list](#)

Figure 43 Queries page.

View FBG data management	
FileName	FBGData2013-3-11 13-06-37.txt
Creation date	2013:03:11 13:06:00
<input type="button" value="Close"/>	

Figure 48 Viewing page.

6.5 Document scanning and system management

The functional modules mainly controlled and managed the basic data which related to the system operation. The system assigned the authority of input data according to the data permission levels of relevant personnel. The integrity and correctness of the data were the basic guarantee of system operation, and the basic data input module provided: **Add**, **Modify**, **Delete** and **Query** functions.

When the system started, FBG data scanning threads and a BOTDR scanning data thread were opened. The scan time was set in the system management module. For the Ripley Landslide, when FBG data scanning threads and BOTDR scanning data were opened, data was monitored using two data scan times set up in the system management module. When the system found a monitoring data file, it saved the FBG results data, BOTDR result data and BOTDR raw data into a database. The user was then able to view or download the data from the platform.

6.6 FBG monitoring time maintenance module

When the FBG system started up, it automatically scanned files according to the specific time, and then stored a file in the database. This Monitoring Time Maintenance module allowed the user to configure the scan time of FBG monitoring data (**Figure 49**). The main operations were **New**, **Modify** and **View**. To enter new values, the “**Append**” button was clicked and a new window popped up (**Figure 50**). Items marked with “*” had to be input. To modify input values, the “**Update**” button corresponding to the item you want to modify was clicked. An Update FBG Monitoring Time pop up window then appeared (**Figure 51**). To view item to be modified, the “**Details**” button corresponding to the item to modify was clicked and a View window popped up (**Figure 52**).

The FBG monitoring time maintenance				
<input type="button" value="Append"/> <input type="button" value="Delete"/>				
No.		Monitoring object	Monitoring time	Function
1	<input type="checkbox"/>	FBG	16:34	<input type="button" value="Details"/> <input type="button" value="Update"/>
2	<input type="checkbox"/>	FBG	07:01	<input type="button" value="Details"/> <input type="button" value="Update"/>

Figure 49 FBG monitoring time maintenance.

AddThe FBG monitoring time maintenance x				
Monitoring objects	FBG			
Monitoring time		Hour		Minute
Remark				
<div> <input type="button" value="Confirm"/> <input type="button" value="Cancel"/> </div>				

Figure 50 Add FBG monitoring time maintenance.

Update FBG monitoring time maintenance x				
Monitoring objects	FBG			
Monitoring time	16	Hour	34	Minute
Remark				
<div> <input type="button" value="Confirm"/> <input type="button" value="Cancel"/> </div>				

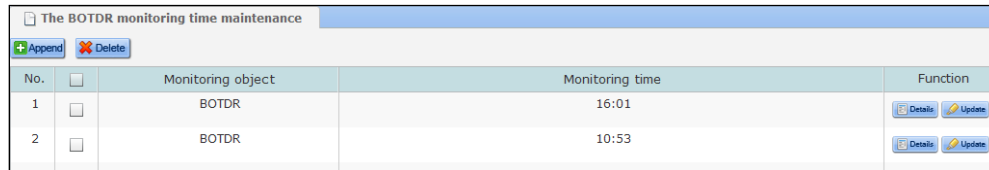
Figure 51 Update FBG monitoring time maintenance.

View FBG monitoring time maintenance x				
Monitoring objects	FBG			
Monitoring time	16	Hour	34	Minute
Remark				
<div> <input type="button" value="Close"/> </div>				

Figure 52 View FBG monitoring time maintenance.

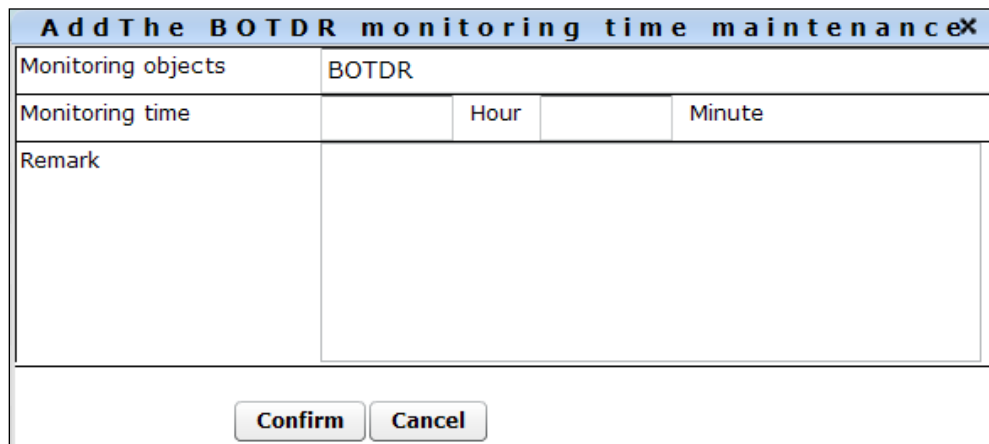
6.7 BOTDR monitoring time maintenance

This module allowed the user to configure the scan time of BOTDR monitoring data (**Figure 53**). The main operations were **New**, **Modify** and **View**. To enter new values, the “**Append**” button was clicked and a new window popped up (**Figure 54**). Items marked with "*" had to be entered. To modify an item, the “**Update**” button corresponding to the item to be modified was clicked. An Update BOTDR Monitoring Time window then popped up (**Figure 55**). Clicking the “**Details**” button corresponding to the item to be modified allowed the user to view the BOTDR Monitoring Time pop up window (**Figure 56**).



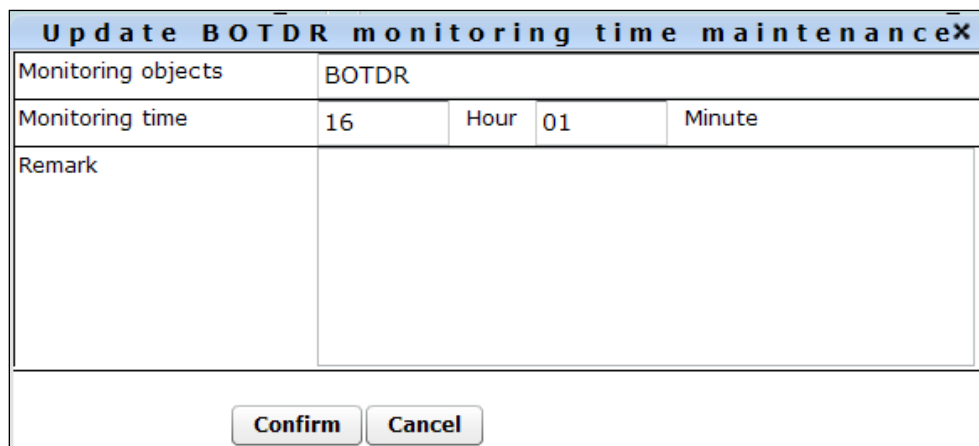
No.	<input type="checkbox"/>	Monitoring object	Monitoring time	Function
1	<input type="checkbox"/>	BOTDR	16:01	<input type="button" value="Details"/> <input type="button" value="Update"/>
2	<input type="checkbox"/>	BOTDR	10:53	<input type="button" value="Details"/> <input type="button" value="Update"/>

Figure 53 BOTDR monitoring time maintenance.



Add The BOTDR monitoring time maintenanceX				
Monitoring objects	BOTDR			
Monitoring time		Hour		Minute
Remark				
<input type="button" value="Confirm"/> <input type="button" value="Cancel"/>				

Figure 54 Add BOTDR monitoring time maintenance.



Update BOTDR monitoring time maintenanceX				
Monitoring objects	BOTDR			
Monitoring time	16	Hour	01	Minute
Remark				
<input type="button" value="Confirm"/> <input type="button" value="Cancel"/>				

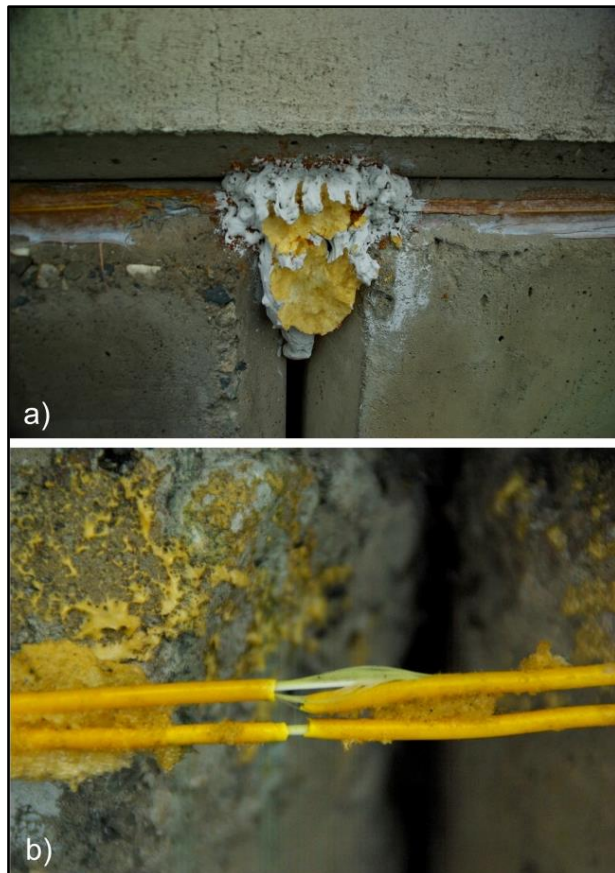
Figure 55 Update BOTDR monitoring time maintenance.

View BOTDR monitoring time maintenance x				
Monitoring objects	BOTDR			
Monitoring time	16	Hour	01	Minute
Remark				
<input type="button" value="Close"/>				

Figure 56 View BOTDR monitoring time maintenance.

6.8 Trouble-shooting FBG and BOTDR instruments at the Ripley Landslide test site

Three months of FBG and BOTDR data were collected for the Ripley Landslide before the installation was damaged by Grizzly Bear activity (**Figure 57**). In addition, epoxy resin and caulking products failed during prolonged intervals of sub-zero temperatures, so that cables no longer attached to the retaining wall in many places by the fall of 2015. Periodic on-site visits



were also required to trouble-shoot hardware, software and telemetry issues. In addition to wildlife, temperature extremes also hindered operations, leading to the failure of the original FBG unit. There were 10 steps to follow when switching out the old and installing the new FBG monitoring demodulation device and testing for damaged fibre-optic cables using the portable OTDR unit (**Table 3; Appendix 4**). The steps followed for repair of fibre-optic cables by welding are presented in **Appendix 5**. For future installations, solutions will be developed during pre-fieldwork technical workshops at CGS and GSC offices.

Figure 57 Damage to the fibre-optic cable: a) Bear claw marks on foam infill; b) damaged cable coatings and exposed optical fibres.

STEP 1 Old Unit

- a) Turn the power **Off**.

STEP 2 Old Unit

- a) Remove the antenna adapter from the antenna interface connector on the panel.
- b) Place protection caps on the antenna interface connector.

STEP 3 New Unit

- a) Remove the protection caps from the antenna interface connector on the panel.
- b) Connect the antenna adapter with the antenna interface connector.

STEP 4 Old Unit

- a) Remove the optical fibre sensor from the optical interface connector on the front panel.
- b) Place the protection caps on the optical interface connector.

STEP 5 New Unit

- a) Remove the protection caps from the optical interface connector.
- b) Clean the optical interface connector with an alcohol sponge.
- c) Wait for alcohol to volatilize, or evaporate, from the optical interface connector.
- d) Connect the adapter connector of the optical fibre sensor to the optical interface connector on the front panel.

STEP 6 New Unit

- a) Connect the mouse with the USB interface connector on the panel: turn **On** wireless mouse.

STEP 7 New Unit

- a) Connect the power line with the 12V INPUT on the panel.

STEP 8 New Unit

- a) Check all connections.
- b) Turn on the power switch.
- c) If working, the power LED should be lit.

STEP 9 New Unit

- a) Optical fibre grating monitoring demodulation software will begin running.

STEP 10 New Unit

- a) When the software test is finished, exit the FBG grating data acquisition system

Table 3 Operational steps for switching out old and installing new FBG monitoring demodulation device.

7. Optical Fibre Sensing Real-Time Monitoring Results and Interpretations

7.1 FBG and BODTR results

The horizontal and vertical FBG displacement sensors detected a gradual and periodic increase in strain following equipment installation in early May 2013. FBG sensor measurement results were strongly influenced by temperature (**Figure 58a**). Displacement amounts totaled 2.5 mm horizontal displacement and 2 mm of vertical displacement from May 2013 to September 2015, with strain rates increasing in October-November 2014, and from November 2014 to February 2015 (**Figure 58b**).

BOTDR monitoring curves for May, June and July 2013 showed a relative shift compared to the initial curve following installation on May 4 2013 (**Figure 59a**). Before going offline, four places with obvious strain were recognized at 1060 m, 1230 m, 1320 m and 1610 m on the retaining wall (**Figure 59b**). Environmental temperatures in August and September of 2013 were too high for the BOTDR monitoring instrument to work properly. Optimal temperatures for functional instrumentation occurred prior to the October 2013 system failure. After this time, strain developed at 780 m destroyed fibre parameters: this position placed the failure point in the buried conduit connecting the array to the bungalow (**Figure 3**).

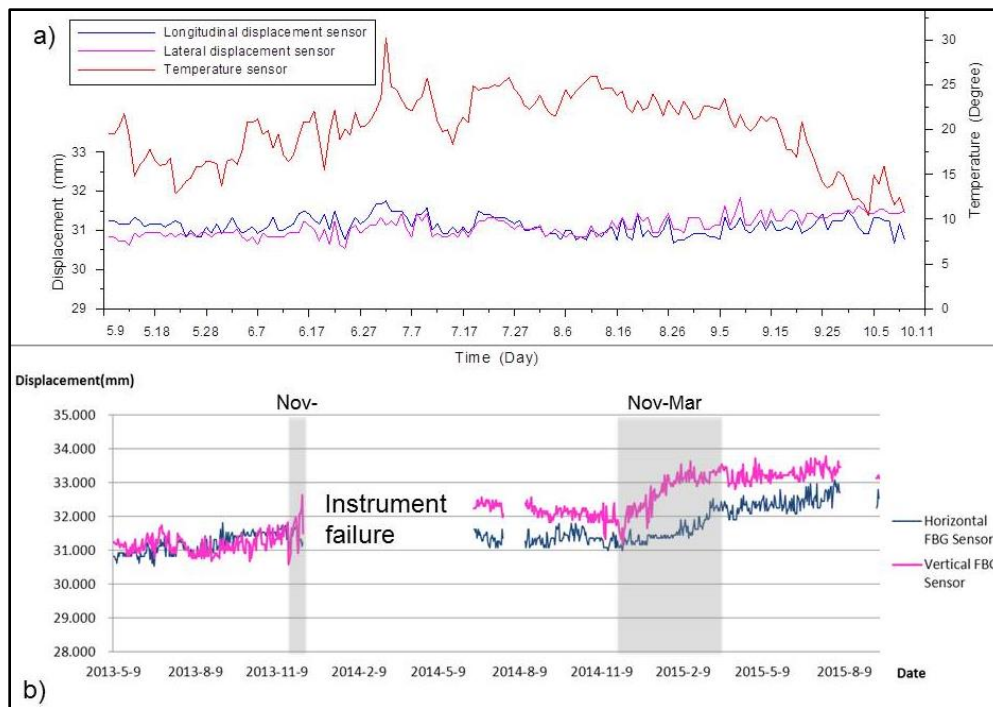


Figure 58 FBG sensor monitoring curves: a) Relationship between temperature and displacement from May 2013 to October 2013 before instrument failure due to cold temperatures starting in November 2013; b) Cumulative horizontal and vertical displacement from May 2013 to August 2015, displacement rates higher during the fall and winter months – greyed areas, data gaps attributed to instrument failure during cold ($< -20^{\circ}\text{C}$) or hot ($> 30^{\circ}\text{C}$) weather periods.

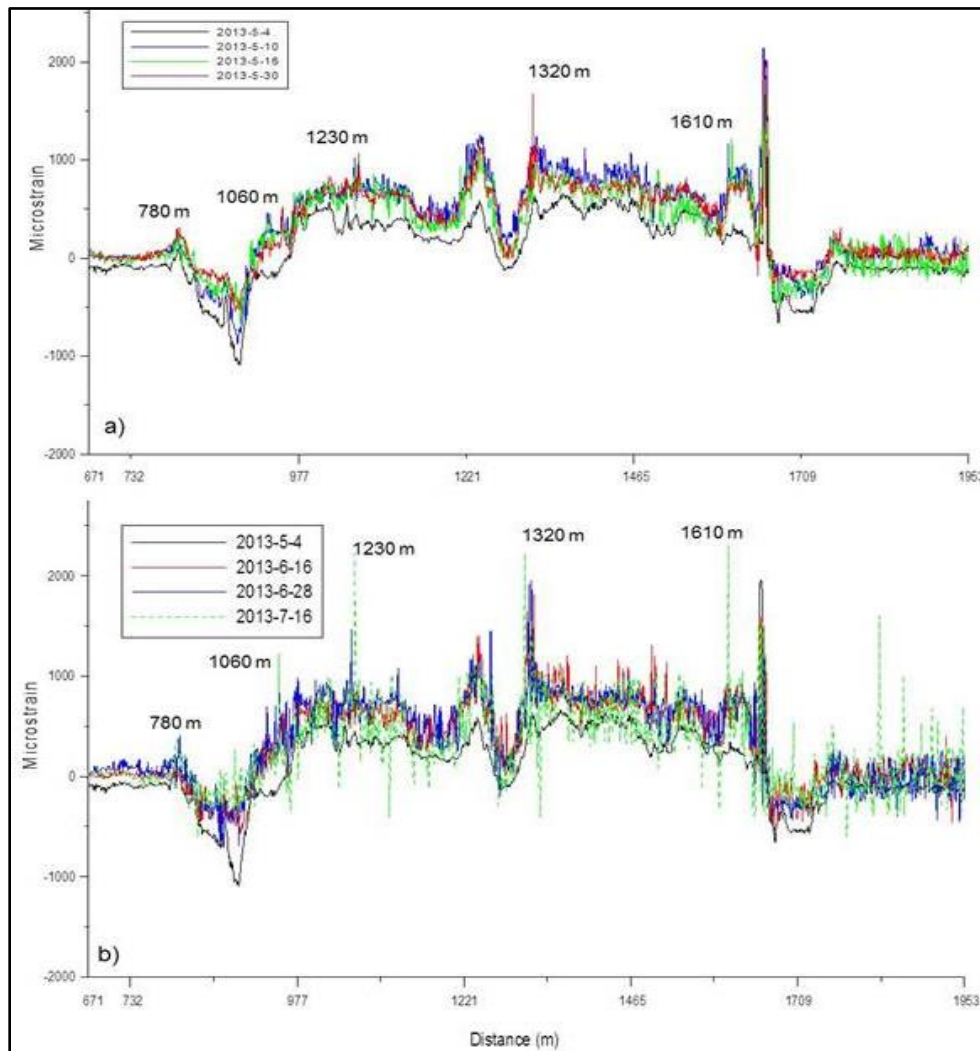


Figure 59 Strain in optical fibre cables detected by BODTR monitoring instrumentation at 780 m, 1060 m, 1230 m, 1320 m and 1610 m: a) data downloaded for May 2013; b) data downloaded for June-July 2013; see Figure 3 for strain locations on the lock-block retaining wall.

7.2 Interpretation of FBG and BODTR data

The FBG and BOTDR systems installed by the CGS and GSC on the lock-block retaining wall separating the CN and CPR tracks provided sporadic real-time monitoring proxy of landslide activity from May 2013 to November 2015 (**Figure 58** and **Figure 59**). Both systems were installed to monitor strain in critical railway infrastructure (**Figure 60**) in response to landslide motion rather than to determine failure mechanism.

Although instrument failures attributed to extreme environmental conditions (e.g., weather conditions, wildlife) and damage during routine track maintenance produced significant data gaps, some trends are observable in the optical fibre sensing real-time monitoring results (**Figure 58** and **Figure 59**). Before going permanently offline in November 2013, BODTR monitoring

identified four places on the retaining wall with obvious strain: at 1060 m, 1230 m, 1320 m and 1610 m (Figure 5). These points likely represent hinge (flexure) lines developing in the retaining wall as it settles into the underlying clay beds (**Figure 60**).

Vertical and horizontal FBG sensors detected displacement of individual blocks over the observation period of less than 2 mm, suggesting the retaining wall remains relatively undeformed as it moves along with a coherent slide block above the shear planes below. FBG sensors captured an increase in displacement rates starting in October-November 2013 (before instrument failure) and between November 2014 and February 2015 (**Figure 3**). This irregular, but cyclical pattern corresponds to higher landslide movement rates in the fall and winter seasons recorded by other monitoring systems (Macciotta et al. 2014; Hendry et al. 2015; Schafer et al. 2015).

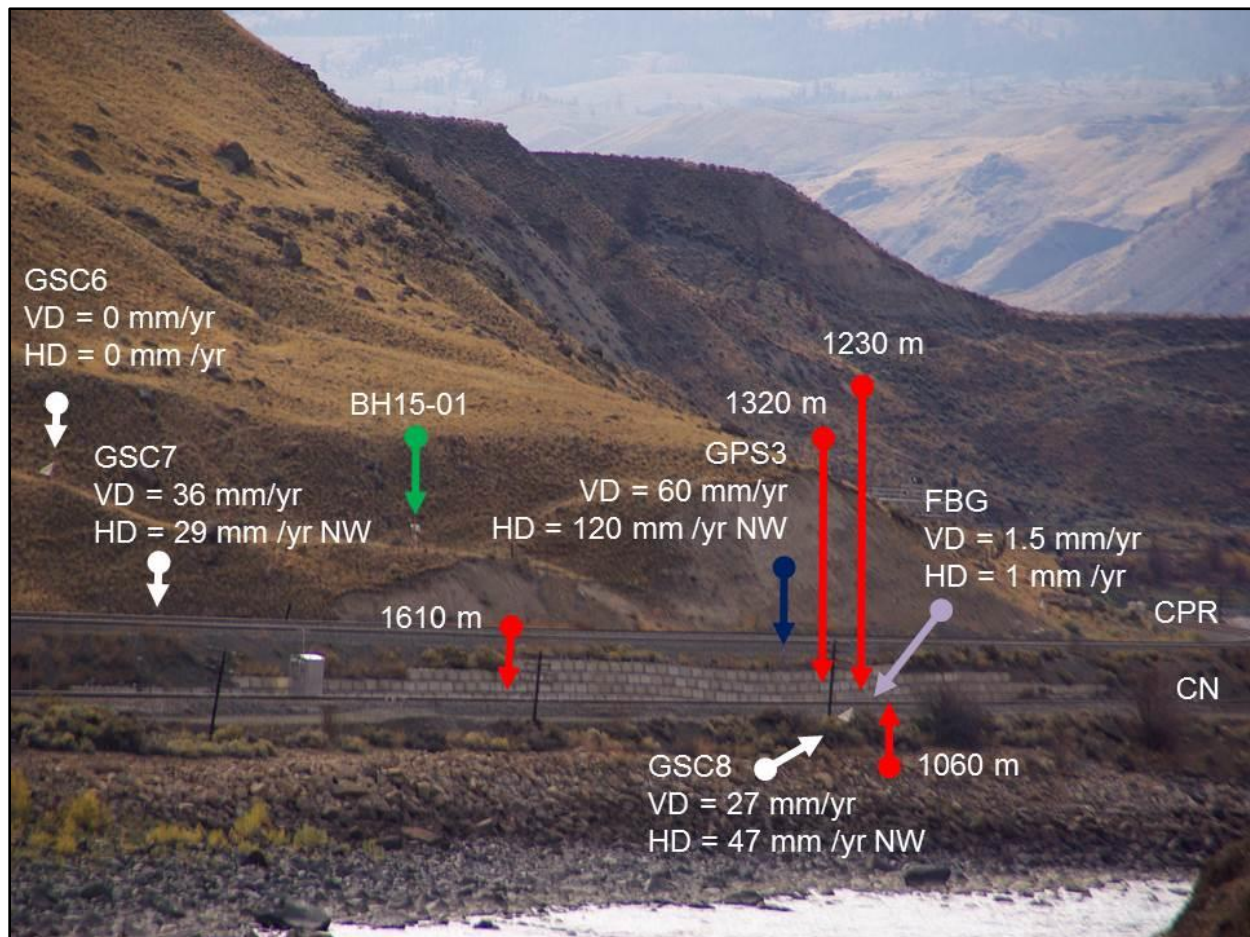


Figure 60 South flank of the Ripley Landslide with sagging retaining wall separating CN and CPR tracks; showing displacement vectors for FBG, GPS and InSAR stations, and strain points detected by BOTDR; VD – vertical displacement; HD – horizontal displacement.

8. Concluding Remarks

8.1 Summary evaluation of fibre-optic cable technologies

FBG and BOTDR technologies detected landslide activity manifesting as small amounts of accumulating strain in the retaining wall and displacement of individual lock blocks. FBG data correlate with other monitoring results and indicate seasonal changes in rate of landslide movement, with peak activity in the fall and winter months. However, in comparison to other technologies employed on-site, the fibre optic data provides no additional information to help characterize the landslide structure and function. Future optical fibre real-time monitoring programs on site (or elsewhere) might apply FBG and BOTDR directly on the landform to evaluate temperature, strain and displacement across surface tension cracks and at depth across shear planes in boreholes.

8.2 Limitations

As installed, both FBG and BOTDR were not reliable monitoring systems for the harsh environmental conditions encountered in the Thompson River valley. Data loss was attributable to failure of experimental hardware and software due to extreme weather events (cold and heat). Cables and sensors were also damaged during track maintenance at several locations on the installation. The systems installed were originally designed to perform in sub-tropical south-east Asia. Clearly, neither functioned as anticipated during experimental design, and future installations should design shielding to protect plastic-coated fibres from grazing animals and railway traffic. The temperature extremes at the test site were also a challenge for heat-sensitive electronic components. Future designs should consider improved insulation, weather-proofing and uninterruptable power supply for Canadian installations. Like all other remote monitoring technologies, on-site access is required to replace failed hardware or reboot corrupted software. For wider adoption of these fibre optic technologies, proprietary software packages with language interfaces for specific countries (e.g., China, Canada) must be developed that are also compatible with commercial programs and devices. Limited internet, cellular or satellite connectivity is another challenge for remote telemetry in mountainous terrain.

8.3 Applications

For small-scale projects like the Ripley Landslide test site, and provided with appropriate resources and safe site access, real-time FBG and BOTDR monitoring arrays can be calibrated, installed and online within 10 days. Training and technical workshops are essential to the maintenance of both systems. Although the fibre optic data was only beneficial to the monitoring the integrity of the lock-block retaining wall, this test case demonstrates that real-time FBG and BOTDR techniques yield complimentary results to data collected by other instrumentation and geophysical testing. If reliability issues can be addressed, fibre optic technologies will offer viable alternative monitoring methods for detecting landslide activity and displacement of railway infrastructure in extreme and remote locations. For example, ruggedized systems with reliable autonomous power sources (e.g., solar panels and battery packs) and data management

(e.g., software and computing hardware) might be suited to alarming for the purposes of track and train safety. Future installation of optical fibre technologies where railways, highways, bridges, pipelines, dams, power transmission lines and buildings are adversely impacted by landslides would ensure the safety and security of critical infrastructure, thereby reducing risks to public safety, the environment, natural resources and the economy.

9. Acknowledgements

This project is the sum of all who have collaborated through research and development, and contributed through science management. Funding through the MOU and oversight by Bai Qin (China Geological Survey) and James Ikkers and David Anderson (NRCAN International Division) ensured that International Collaboration was seamlessly pursued. Research funding by Transport Canada was managed by Sharon Philpott (2014-Present) and Merrina Zhang (2013-2014) Transport Canada) Carmel Lowe, Adrienne Jones and Philip Hill (GSC-Sidney) provided direction and approval for activities. Wendy Sladen (GSC-Ottawa) and Lionel Jackson (GSC-Vancouver) helped with the field installation of monitoring systems in April-May 2013. From CGS-CHEGS, Zhang Qing, Shi Yanxin, Zhang Xiaofei, Lv Zhonghu, Hao Wenjie, Meng Xianwei, Jiang Fan and Hao Shuli were instrumental in compilation of technical materials, training and installation of the FBG and BODTR monitoring arrays at the Ripley Landslide. Danial Mariampillai (GSC-Sidney) critically reviewed this Open File.

10. References





- Bobrowsky, P., Sladen, W., Huntley, D., Qing, Z., Bunce, C., Edwards, T., Hendry, M., Martin, D., and Choi, E. (2014) Multi-parameter monitoring of a slow-moving landslide: Ripley Landslide, British Columbia, Canada. In Proceedings of the International Association of Engineering Geologists, 5 p., Turin, Italy
- Bunce, C. and Chadwick, I. (2012) GPS monitoring of a landslide for railways. In Eberhardt et al. (Editors), Landslides and Engineered Slopes: Protecting Society through Improved Understanding, pp. 1373-1379
- Hendry, M., Macciotta, R. and Martin, D. (2015) Effect of Thompson River elevation on velocity and instability of Ripley Slide. Canadian Geotechnical Journal, Vol. 52(3), pp. 257-267
- Hoepffner, R., Singer, J., Thuro, K. and Aufleger, M. Development of an integral system for dam and landslide monitoring based on distributed fibre optic technology. Ensuring reservoir safety into the future, 13 p., Thomas Telford, London

- Huafu, P., Peng C., Jianhua Y, Honghu Z., Xiaoqing C., Laizheng P, and Dongsheng X. (2011) Monitoring and warning of landslides and debris flows using an optical fibre sensor technology. *Journal of Mountain Science* 8 (5), pp. 728-738
- Huang A-B., Lee, J-T., Ho, Y-T., Chiu, Y-F., Chen, S-Y. (2012) Stability monitoring of rainfall-induced deep landslides through pore pressure profile measurements. *Soils and Foundations*, Vol. 52 (4), pp. 737-747, Japanese Geotechnical Society
- Huang C-J, Chu, C-R, Ping-Sen and Chen P-S (2002) Calibration and Deployment of a Fibre-Optic Sensing System for Monitoring Debris Flows. *Sensors* 12, pp. 5835-5849.
- Huntley, D. and Bobrowsky, P. (2014a) Surficial geology and monitoring of the Ripley Slide, near Ashcroft, British Columbia, Canada; Geological Survey of Canada, Open File 7531, 21 p.
- Huntley, D., Bobrowsky, P., Zhang, Q., Sladen W., Bunce, C., Edwards, T, Hendry, M., Martin, D., and Choi, E. (2014b) Fibre optic strain monitoring and evaluation of a slow-moving landslide near Ashcroft, British Columbia, Canada; *Proceedings of World Landslide Forum 3*, 6 p. Beijing, China
- Huntley, D., Bobrowsky, P., Zhang, Q., Zhang, X., Lv, Z., Hendry, M., Macciotta, R., Schafer, M., Le Meil, G., Journault, J. and Tappenden, K. (2016) Application of Optical Fibre Sensing Real-Time Monitoring Technology at the Ripley Landslide, near Ashcroft, British Columbia, Canada. *Proceedings Volume, Canadian Geotechnical Society, GeoVancouver2016 Annual Meeting*, 13 pages
- Huntley, D., Bobrowsky, P., Parry, N., Bauman, P., Candy, C. and Best, M. (2017a) Ripley Landslide: the geophysical properties of a slow-moving landslide near Ashcroft, British Columbia, Canada; Geological Survey of Canada, Open File 8062, 63 pages
- Huntley, D., Bobrowsky, P. and Best, M. (2017b) Combining terrestrial and waterborne geophysical surveys to investigate the internal composition and structure of a very slow-moving landslide near Ashcroft, British Columbia, Canada. In: *Landslide Research and Risk Reduction for Advancing Culture and Living with Natural Hazards*, 4th World Landslide Forum (ICL-IPL), Ljubljana, Slovenia 29- May 2 June 2017, Volume 2, 15 p. Springer Nature
- Huntley, D., Bobrowsky, P., Charbonneau, F., Journault, J. and Hendry, M. (2017c) Innovative landslide change detection monitoring: application of space-borne InSAR techniques in the Thompson River valley, British Columbia, Canada. In: *Landslide Research and Risk Reduction for Advancing Culture and Living with Natural Hazards*, 4th World Landslide Forum (ICL-IPL), Ljubljana, Slovenia 29- May – 2 June 2017, Volume 3, 13 p. Springer Nature
- Laudati A., Mennella F., Esposito M., Cusano A., Giordano M., Breglio G., Sorge S., Calisti Tassini C., Torre A., D'Altrui G. and Cutolo A. (2007) A fibre optic Bragg grating seismic sensor. In: *SPIE Proceedings on Optical Fibre Sensors* 6619.

- Macciotta, R., Hendry, M., Martin, D., Elwood, D., Lan, H., Huntley, D., Bobrowsky, P. , Sladen, W, Bunce C., Choi, E and Edwards, T. (2014) Monitoring of the Ripley Slide in the Thompson River Valley, B.C. Proceedings of Geohazards 6 Symposium, Kingston, Ontario, Canada
- Schafer, M., Macciotta, R., Hendry, M., Martin, D., Bunce, C. and Edwards, T. (2015) Instrumenting and Monitoring a Slow Moving Landslide. GeoQuebec 2015 Paper, 7 p.
- Wang, B-J., Li, K., Shi B. and Wei, G-Q. (2008) Test on application of distributed fibre optic sensing technique into soil slope monitoring. Landslides 6 (1), pp. 61-68
- Wang ,F., Zhang Y., Huo, Z. and Peng, X. (2009) Monitoring on Shuping Landslide in the Three Gorges Dam Reservoir, China. In Wang, F and Li, T. (eds.) Landslide Disaster Mitigation in Three gorges Reservoir, China, pp. 257-273, Springer, Berlin
- Xu, L., Li S., Liu,X and Feng C. (2007) Application of real-time telemetry technology to landslide in Tianchi Fengjie of Three Gorges Reservoir Region. Chinese Journal of Rock Mechanics and Engineering
- Yong, D., Bin, S., He-liang, C., Wen-bin, S. and Jie L. (2005) A fibre optic sensing net applied in slope monitoring based on Brillouin scattering. Chinese Journal of Geotechnical Engineering 2005-03
- Yoshida, Y., Kashiwai, Y, Murikami, E., Ishida, S. and Hashiguchi, N. (2002) Development of the monitoring system for slope deformations with fibre Bragg grating arrays. In: SPIE Proceedings 4694, Smart Structures and Materials 2002: Smart Sensor Technology and Measurement Systems 296
- Zhang, X., Lv, Z., Meng, X., Jiang, F. and Zhang, Q. (2014) Application of Optical Fibre Sensing Real-Time Monitoring Technology Using the Ripley Landslide. Applied Mechanics and Materials, Vol. 610, pp. 199-204.

APPENDIX 1

Detailed list of items for the China-Canada optical fibre real-time monitoring project

Item	尺寸 (长×宽×高mm) Size (length*width*height)	物件名称 Description	数量 Quantity	备注 Remark
1	650*450*270	FBG仪器主机 FBG instrument	1	
		鼠标、键盘 Mouse & keyboard	1	
		220转12V电源适配器 power adapter	1	
2	430*290*260	黄色光纤 fibre	1	
3	430*330*200	光纤熔接机及配件 Optical fibre welding machine and accessories	1	
4	370*260*150	OTDR仪器 OTDR instrument	1	

APPENDIX 2

Fibre Bragg Grating Installation and Operation: Quick View

FBG Sensors and Fibre-Optic Cable

- 1) Vertical and horizontal FGB sensors were installed at the Ripley Landslide
- 2) Measured strain, temperature, and force and temperature by analyzing the back-scatter of laser light in specific frequencies
- 3) As force changes, the wavelength of light carried by the FOC changes (ODTR unit tests this function)

Fault Analysis

- 1) If the FOC is damaged, then FBG sensors (and BODTR) will not receive information (ODTR unit tests for this)

SERVER Instructions

- 1) Located under FBG (and BODTR) units in bungalow
- 2) Ensure power cables are connected
- 3) Open panel; press **Green Button**
- 4) Close panel
- 5) Central Computer password: **shddzx!dzjc!Zjhz2013Server**

Data monitoring platform

<http://173.182.75.78:8080/Datamonitor/DXKS.html>

User Name: **esscgs**

Password: **esscgs**

Fault Analysis

- 1) Reboot computer and pull out and re-insert cable to Sierra wireless modem

Turning Off Old FBG Unit

- 1) Check to see if Server unit is **On**
- 2) Switch **Off** Power Button on FBG unit
- 3) Unplug Power Cable for FBG unit from Power Bar
- 4) Unplug 12V cable from FBG unit
- 5) Unplug antenna
- 6) Unplug fibre-optic cable (FOC) from FC/APC port
- 7) Place clear plastic cap on exposed FOC tip; red cap on AC/APC port
- 8) Unplug RS 232 cable
- 9) Unplug mouse from FBG unit

Turning On New FBG Unit

- 1) Turn on wireless keyboard and mouse
- 2) Plug in RS 232 cable
- 2) Remove red cap from FC/APC port
- 3) Remove clear plastic cap from FOC; clean with alcohol; wait 1 minute
- 4) Insert cleaned FOC into FC/APC port
- 5) Plug in 12V cable into FBG unit
- 6) Plug in antenna
- 7) Check connection to Power Adapter
- 7) Plug Power Cable into Power Bar (use plug adapter)
- 8) Turn **On** FBG unit and run installed software

APPENDIX 3
Brillouin Optical Time Domain Reflectometry
Installation and Operation: Quick View

BODTR and Fibre-Optic Cable

FOC

- 1) There was an excess of unused FOC at both ends of the BODTR unit (dead zones)
- 2) 100 m was required to measure backscatter
- 3) 400 m was required for reference (with no strain)

Fault Analysis

- 1) If the FOC is damaged, then BODTR unit will not receive information
- 2) Check cable, inventory damage and take photographs

BOTDR operation steps

- 1) Connect all power lines
- 2) At the same time, connect serial line and network cable between BOTDR and the server
- 2) Open the server to execute MyQQ.exe application programs
- 3) Start the BOTDR unit by powering on; unit will be on standby until acquisition time is set
- 4) After collection, data is transmitted to the Server
- 5) To analyse, download relevant strain data by remote access from the Server website

APPENDIX 4

Optical Time Domain Reflectometry Repair Operation: Quick View

ODTR Operation

- 1) Take photo of unit (in place) before doing anything; email to CHEGS
- 2) Turn on ODTR unit
- 3) Remove the fibre-optic cable (FOC) from BODTR unit; place red cap on exposed port
- 3) Clean FOC tip with alcohol; plug into **Port 1** on OTDR unit
- 4) Press **F1** (OTDR function on display panel)
- 5) Press **AVERAGE**
- 6) Press **SETUP** button
- 7) Press "**Real Time**" button
- 8) Press **F1**; select 1550 nm (wavelength of transmitted light)
- 9) The press **ENTER**
- 10) Press **F2**, scroll down and select **5 km** for distance
- 11) Then press **AVERAGE** (peak will show where cable is compromised)
- 12) For better resolution select **1 km**
- 13) If an ERROR message and a red screen appears, press **ESC**

Fault Analysis

- 1) For FBG and BODTR, check both ends of the FOC
- 2) For BODTR, total FOC length is 2430 m
- 3) If reading anomalies on ODTR are <903 m or > 1647 m, then FOC damage is in the conduit
- 4) Take SD card and adapter; email CHEGS

APPENDIX 5

Welding Fibre-Optic Cable Operation: Quick View

WELDING FIBRE OPTIC CABLE Operation

Important

FOC were unplugged from BODTR or FGB units before welding

- 1) Outer coating incrementally cut with 2.0 pliers at 15 cm from end
- 2) Outer fibres trimmed off with scissors
- 3) Shrink wrap added (enough for 30 welds or 15 breaks)
- 4) A second pliers (inner) used to incrementally trim off inner plastic coating at 3 cm
- 5) Surfaces cleaned with alcohol
- 6) Trimming tool was opened and cleaned out with air can
- 7) End of white sheath were lined up at 15
- 8) Lid was closed, button pressed
- 9) This turned on welding unit
- 10) Bare end placed in unit, then align so fibre was between tips
- 11) Steps 1-10 were repeated for other end
- 12) Yellow button was pressed and then waited for weld
- 13) Shrink wrap was moved over welded joint
- 14) Welding unit had enough power for 3 hours of welding before recharging needed

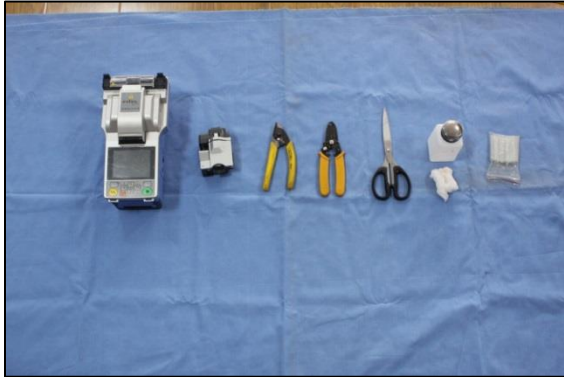
Fault Analysis

- 1) Monitor times were before 11.00 am and between 11.30 am and 2.30 pm

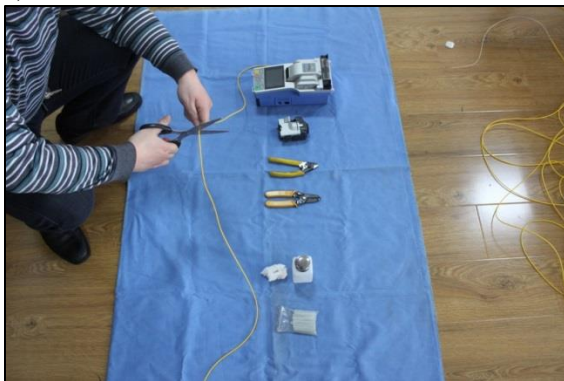
Welding Fibre-Optic Cables

The following sequence of figures shows the process of replacing damaged fibre optic cable and repairing by welding undamaged cable.

1) ALL tools used in the process



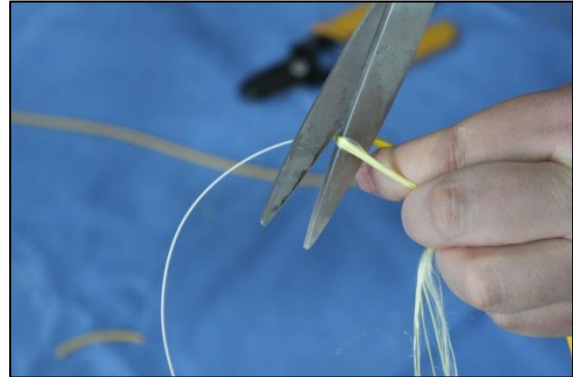
2) Fibre cut with scissors



3) Yellow coating layer removed using 2.0 AWG notches (15 cm length cut in two lengths)



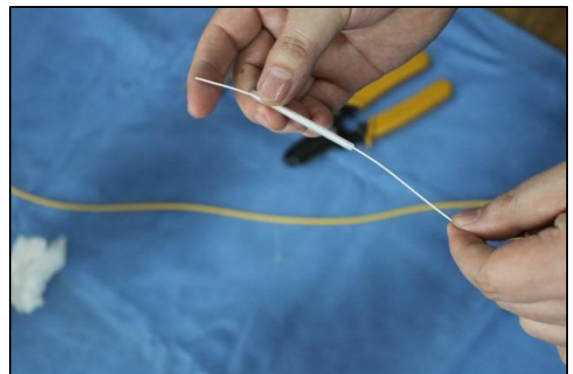
4) Silk cladding cut



5) Exposed inner white coat and cable length was 15 cm



6) Heat shrink tubing slid over white coat and cable



7) Removed 3 cm of white plastic coat (1.5 cm at a time)



8) Exposed 3 cm of fibre-optic cable



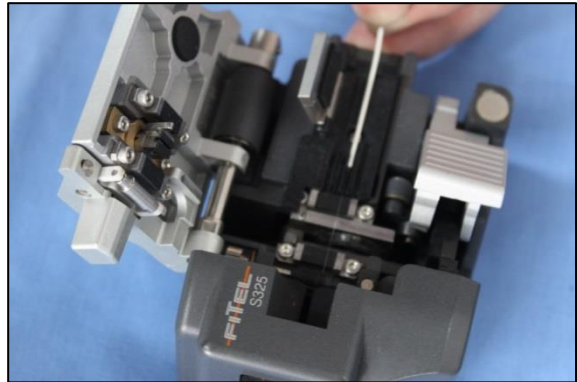
9) Cleaned the fibre core with cotton soaked in alcohol



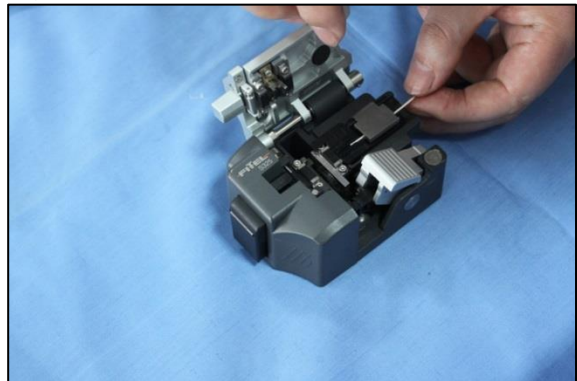
10) Cutting knife opened



11) Damaged fibre placed into the cutting knife



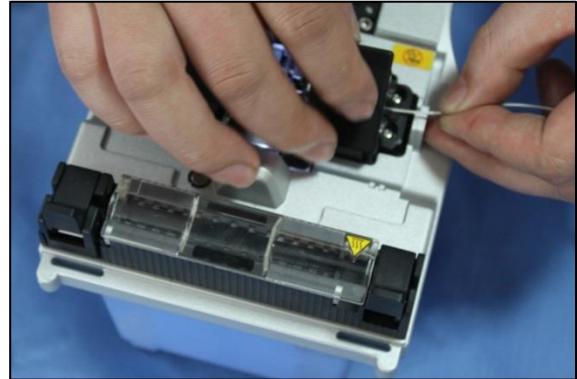
12) Fibre secured



13) Fibre cut



16) Fibre secured

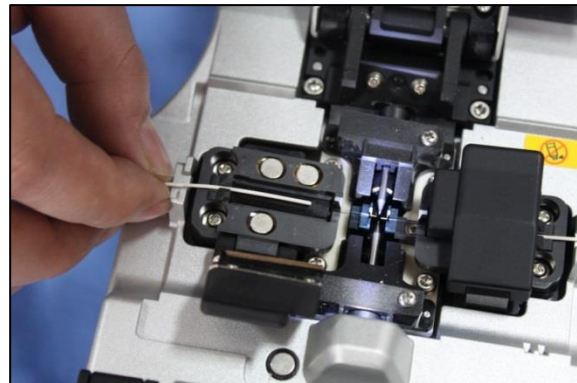


14) Red button pressed to power on the welding machine

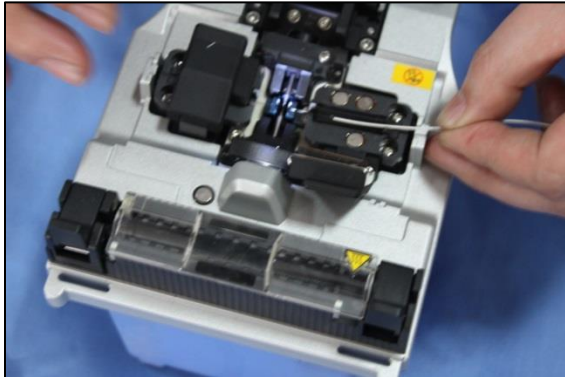


17) Prepare second fibre following steps 3-16 except step 6 (no heat shrink needed)

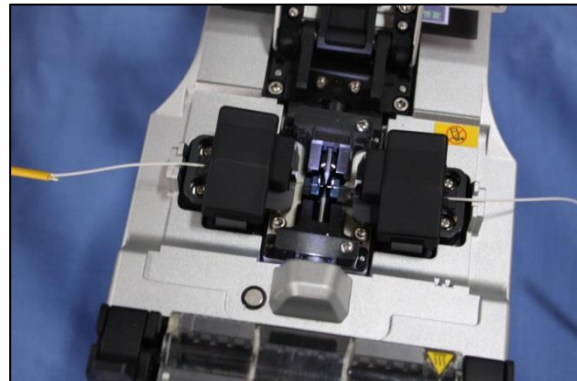
18) The second fibre placed in the welding machine



15) Fibre placed in the welding machine



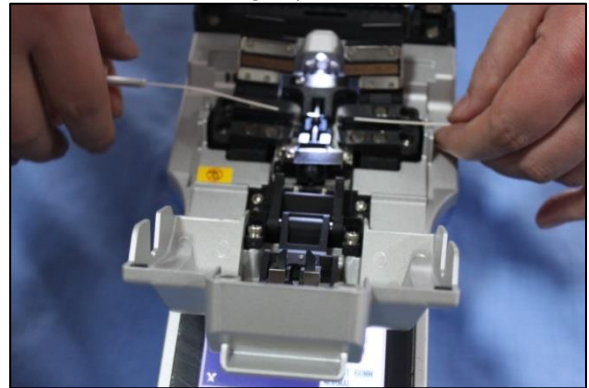
19) Second fibre secured



20) Green button pressed



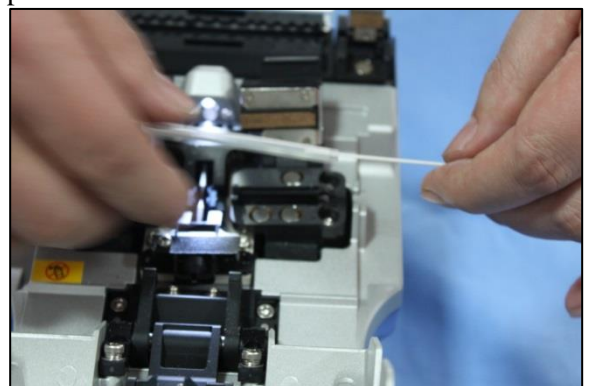
21) Fibre removed lightly



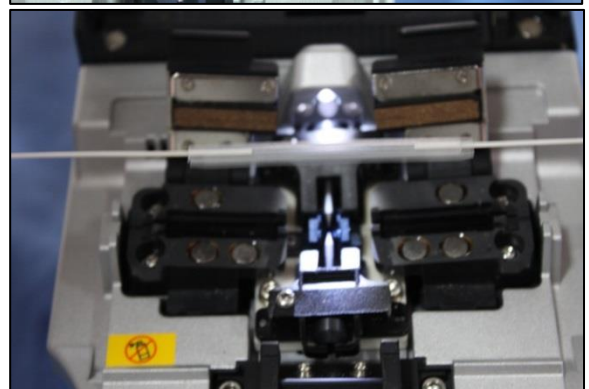
21) Welding started (note microscopic view of cables being welded)



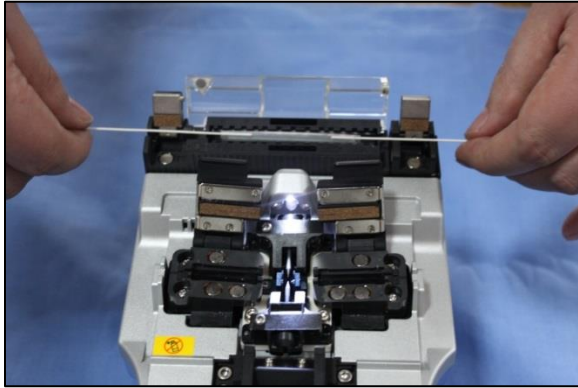
22) Heat shrink tubing moved to the welding point



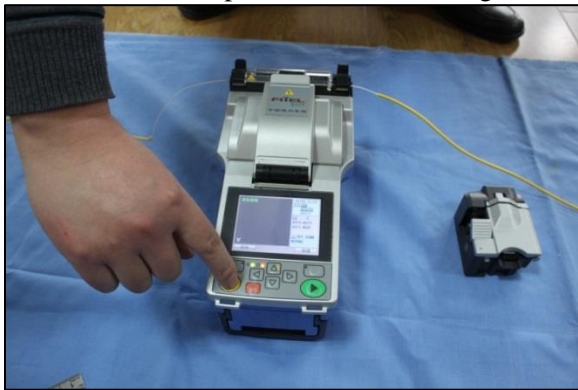
22) When welding was complete, a display read 0.0db—0.05db is OK



23) Fibre placed in the heating element



24) Yellow button pressed to start heating



25) Cooled and newly welded fibre-optic cable to be tested in the portable OTDR unit



